



# Algebraic Domain Decomposition Solvers for Large-Scale Problems Using Graph Techniques

---

Alexander Heinlein<sup>1</sup>

Graphs&Data@TUDelft Seminar, Delft University of Technology, April 3, 2025

<sup>1</sup>Delft University of Technology

## 1 Introduction to Schwarz Domain Decomposition Methods

## 2 The FROSch Package – Algebraic and Parallel Schwarz Preconditioners in TRILINOS

Based on joint work with

**Axel Klawonn**

**Siva Rajamanickam**

**Oliver Rheinbach and Friederike Röver**

**Olof Widlund**

(University of Cologne)

(Sandia National Laboratories)

(TU Bergakademie Freiberg)

(New York University)

## 3 Some Challenging Application Problems

Based on joint work with

**Filipe Cumaru and Hadi Hajibeygi**

**Axel Klawonn, Jascha Knepper, and Lea Saßmannshausen**

**Mauro Perego and Siva Rajamanickam**

**Oliver Rheinbach**

**Kathrin Smetana**

**Olof Widlund**

(Delft University of Technology)

(University of Cologne)

(Sandia National Laboratories)

(TU Bergakademie Freiberg)

(Stevens Institute of Technology)

(New York University)

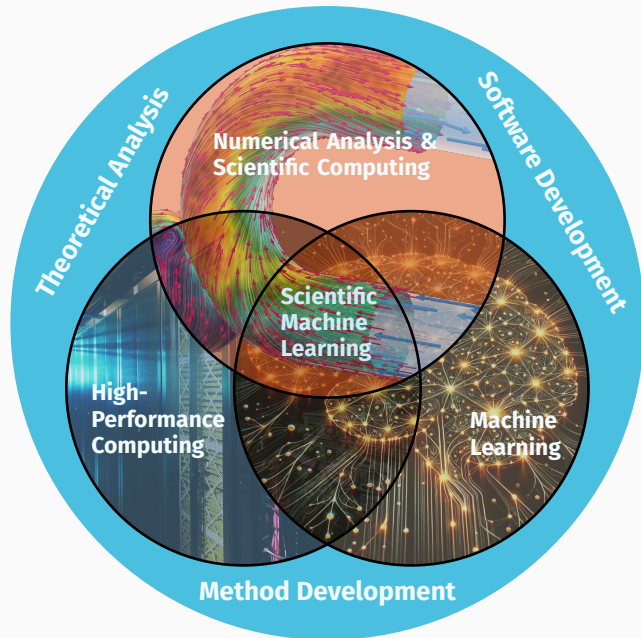
## 4 Learning Extension Operators Using Graph Neural Networks

Based on joint work with

**Siva Rajamanickam and Ichitaro Yamazaki**

(Sandia National Laboratories)

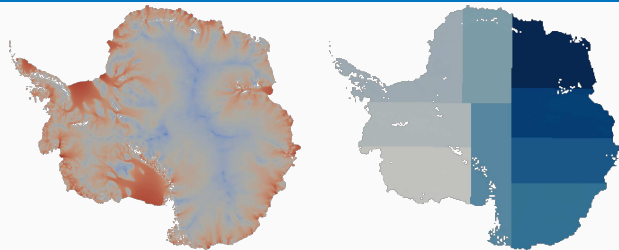
# SCaLA – Scalable Scientific Computing and Learning Algorithms



# **Introduction to Schwarz Domain Decomposition Methods**

---

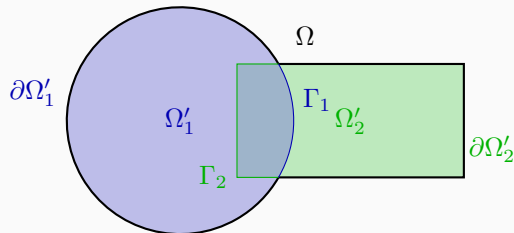
# Domain Decomposition Methods



Graphics based on results from [Heinlein, Perego, Rajamanickam \(2022\)](#)

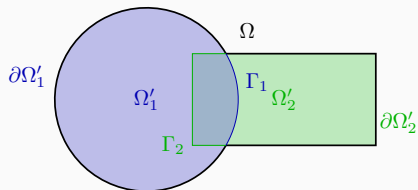
**Historical remarks:** The **alternating Schwarz method** is the earliest **domain decomposition method (DDM)**, which has been invented by **H. A. Schwarz** and published in **1870**:

- Schwarz used the algorithm to establish the **existence of harmonic functions** with prescribed boundary values on **regions with non-smooth boundaries**.



# The Alternating Schwarz Algorithm

For the sake of simplicity, instead of the two-dimensional geometry,



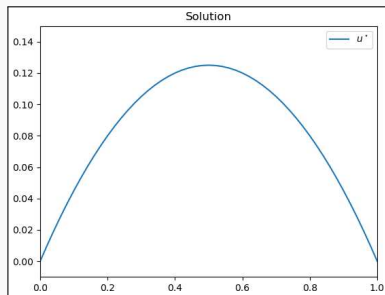
we consider the **one-dimensional Poisson equation**

$$\begin{aligned} -u'' &= 1 \quad \text{in } [0, 1], \\ u(0) &= u(1) = 0. \end{aligned}$$

**Overlapping domain decomposition:**



**Solution:**  $u(x) = -\frac{1}{2}x(x-1).$



# The Alternating Schwarz Algorithm – 1D Laplace Results

Let us consider the simple boundary value problem: Find  $u$  such that

$$-u'' = 1, \text{ in } [0, 1], \quad u(0) = u(1) = 0$$

We perform an **alternating Schwarz iteration**:

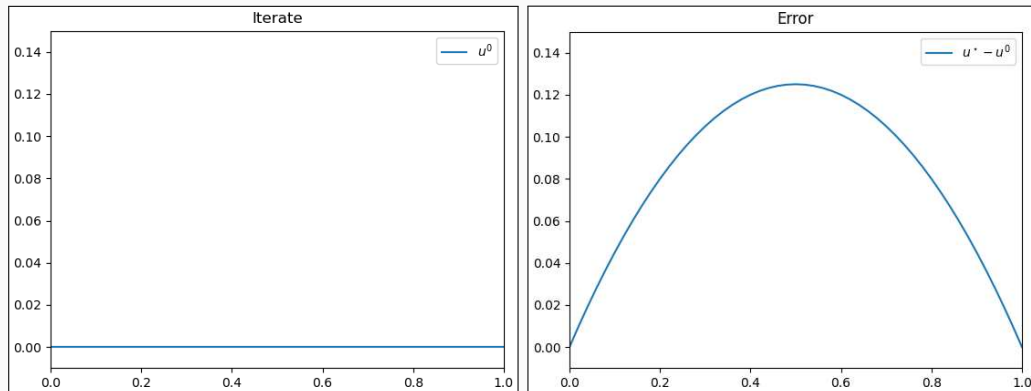


**Figure 1:** Iterate (left) and error (right) in iteration 0.

# The Alternating Schwarz Algorithm – 1D Laplace Results

Let us consider the simple boundary value problem: Find  $u$  such that

$$-u'' = 1, \text{ in } [0, 1], \quad u(0) = u(1) = 0$$

We perform an **alternating Schwarz iteration**:

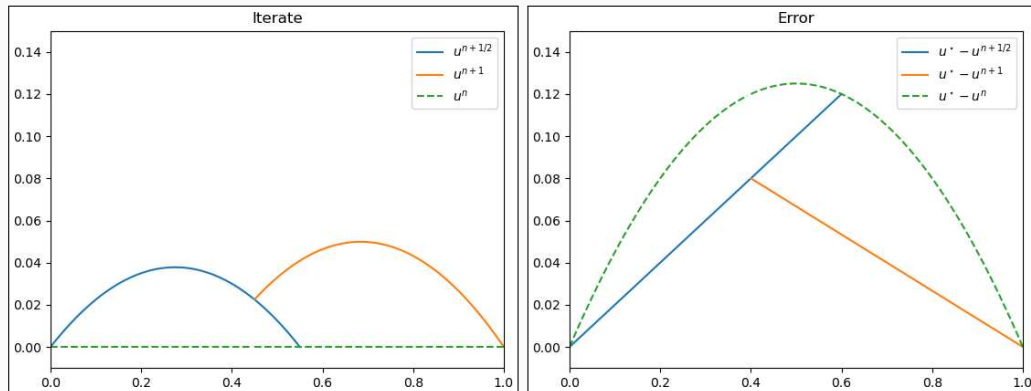


**Figure 1:** Iterate (left) and error (right) in iteration 1.

# The Alternating Schwarz Algorithm – 1D Laplace Results

Let us consider the simple boundary value problem: Find  $u$  such that

$$-u'' = 1, \text{ in } [0, 1], \quad u(0) = u(1) = 0$$

We perform an **alternating Schwarz iteration**:

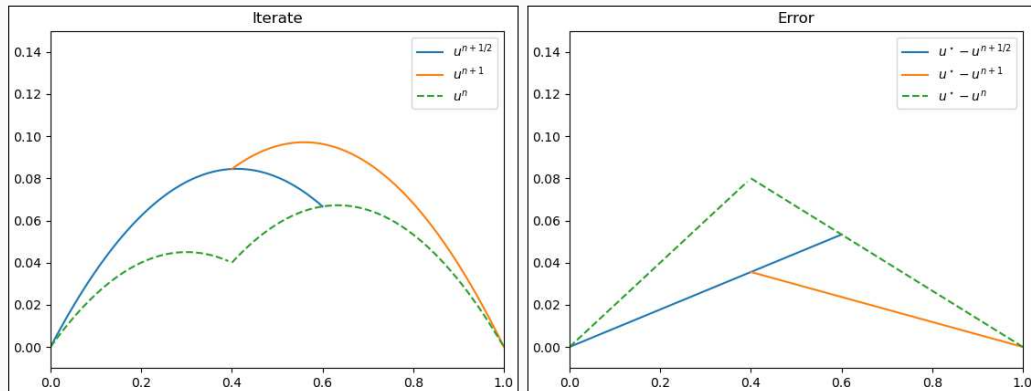


**Figure 1:** Iterate (left) and error (right) in iteration 2.

# The Alternating Schwarz Algorithm – 1D Laplace Results

Let us consider the simple boundary value problem: Find  $u$  such that

$$-u'' = 1, \text{ in } [0, 1], \quad u(0) = u(1) = 0$$

We perform an **alternating Schwarz iteration**:

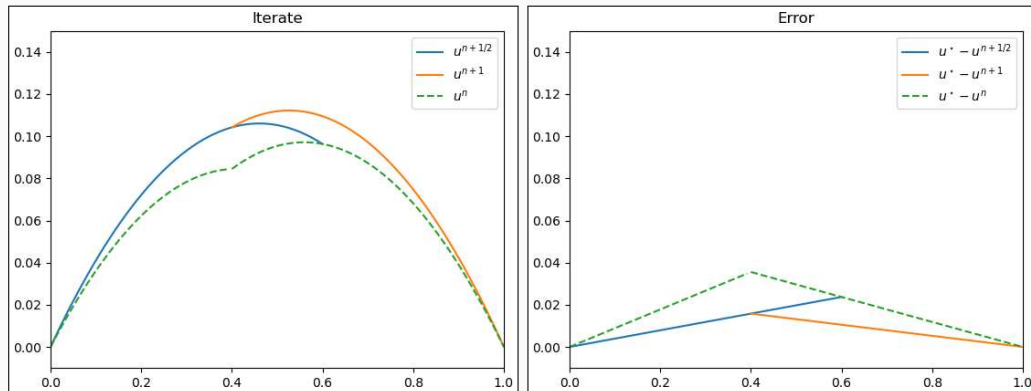


**Figure 1:** Iterate (left) and error (right) in iteration 3.

# The Alternating Schwarz Algorithm – 1D Laplace Results

Let us consider the simple boundary value problem: Find  $u$  such that

$$-u'' = 1, \text{ in } [0, 1], \quad u(0) = u(1) = 0$$

We perform an **alternating Schwarz iteration**:

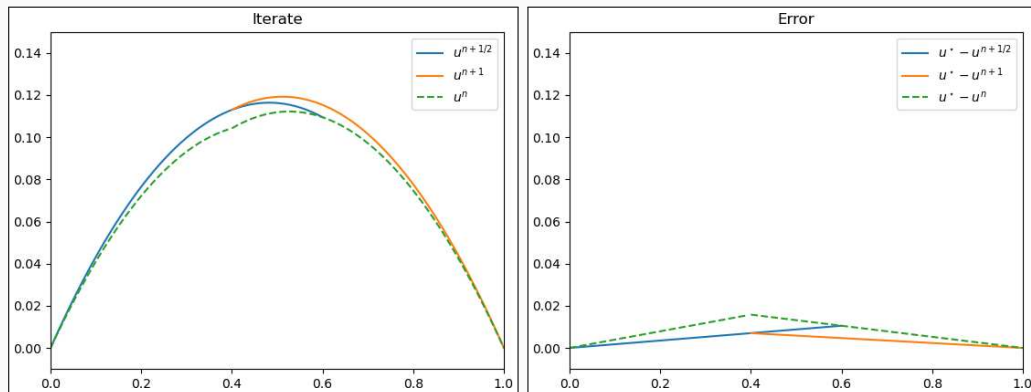


**Figure 1:** Iterate (left) and error (right) in iteration 4.

# The Alternating Schwarz Algorithm – 1D Laplace Results

Let us consider the simple boundary value problem: Find  $u$  such that

$$-u'' = 1, \text{ in } [0, 1], \quad u(0) = u(1) = 0$$

We perform an **alternating Schwarz iteration**:

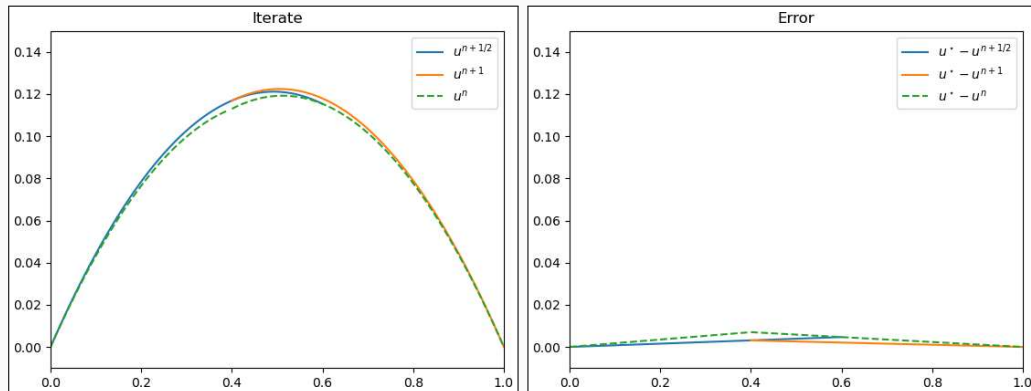


**Figure 1:** Iterate (left) and error (right) in iteration 5.

# Sequential Nature of the Alternating Schwarz Algorithm

The alternating Schwarz algorithm is **sequential** because **each local boundary value problem** depends on the solution of the **previous Dirichlet problem**:

$$(D_1) \begin{cases} -\Delta u^{n+1/2} = f & \text{in } \Omega'_1, \\ u^{n+1/2} = \mathbf{u}^n & \text{on } \partial\Omega'_1 \\ u^{n+1/2} = \mathbf{u}^n & \text{on } \Omega \setminus \overline{\Omega'_1} \end{cases}$$

$$(D_2) \begin{cases} -\Delta u^{n+1} = f & \text{in } \Omega_2, \\ u^{n+1} = \mathbf{u}^{n+1/2} & \text{on } \partial\Omega'_2 \\ u^{n+1} = \mathbf{u}^{n+1/2} & \text{on } \Omega \setminus \overline{\Omega'_2} \end{cases}$$



**Idea:** For all red terms, we use the values from the previous iteration. Then, the both Dirichlet problem can be solved at the same time.

# Sequential Nature of the Alternating Schwarz Algorithm

The alternating Schwarz algorithm is **sequential** because **each local boundary value problem** depends on the solution of the **previous Dirichlet problem**:

$$(D_1) \begin{cases} -\Delta u^{n+1/2} = f & \text{in } \Omega'_1, \\ u^{n+1/2} = \mathbf{u}^n & \text{on } \partial\Omega'_1 \\ u^{n+1/2} = \mathbf{u}^n & \text{on } \Omega \setminus \overline{\Omega'_1} \end{cases}$$

$$(D_2) \begin{cases} -\Delta u^{n+1} = f & \text{in } \Omega_2, \\ u^{n+1} = \mathbf{u}^{n+1/2} & \text{on } \partial\Omega'_2 \\ u^{n+1} = \mathbf{u}^{n+1/2} & \text{on } \Omega \setminus \overline{\Omega'_2} \end{cases}$$



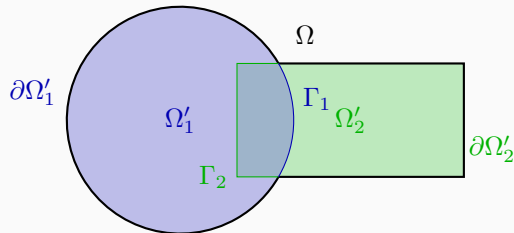
**Idea:** For all red terms, we **use the values from the previous iteration**. Then, the both Dirichlet problem **can be solved at the same time**.

# The Parallel Schwarz Algorithm

The **parallel Schwarz algorithm** has been introduced by **Lions (1988)**. Here, we solve the local problems

$$(D_1) \begin{cases} -\Delta u_1^{n+1} = f & \text{in } \Omega'_1, \\ u_1^{n+1} = u_2^n & \text{on } \partial\Omega'_1, \end{cases}$$

$$(D_2) \begin{cases} -\Delta u_2^{n+1} = f & \text{in } \Omega_2, \\ u_2^{n+1} = u_1^n & \text{on } \partial\Omega'_2. \end{cases}$$



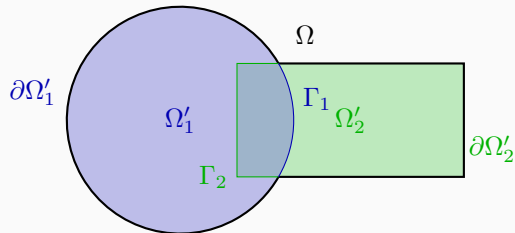
Since  $u_1^n$  and  $u_2^n$  are both computed in the previous iteration, the problems can be solved independent of each other.

# The Parallel Schwarz Algorithm

The **parallel Schwarz algorithm** has been introduced by **Lions (1988)**. Here, we solve the local problems

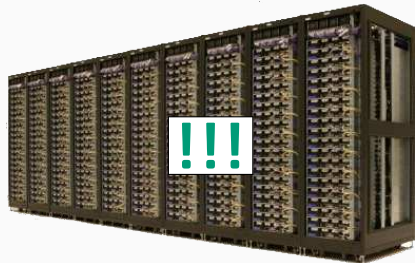
$$(D_1) \begin{cases} -\Delta u_1^{n+1} = f & \text{in } \Omega'_1, \\ u_1^{n+1} = u_2^n & \text{on } \partial\Omega'_1, \end{cases}$$

$$(D_2) \begin{cases} -\Delta u_2^{n+1} = f & \text{in } \Omega_2, \\ u_2^{n+1} = u_1^n & \text{on } \partial\Omega'_2. \end{cases}$$



Since  $u_1^n$  and  $u_2^n$  are both computed in the previous iteration, the problems can be solved independent of each other.

This method is suitable for **parallel computing!**



# The Parallel Schwarz Algorithm – 1D Laplace Results

Let us again consider the simple boundary value problem: Find  $u$  such that

$$-u'' = 1, \text{ in } [0, 1], \quad u(0) = u(1) = 0.$$

We perform a **parallel Schwarz iteration**:

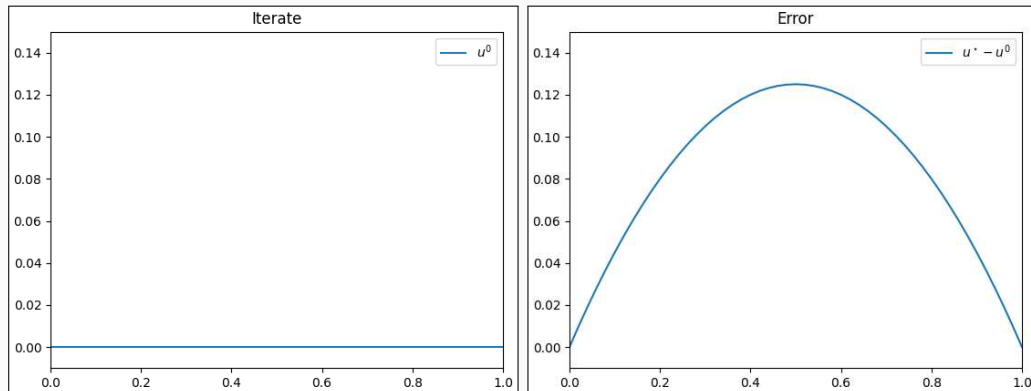


**Figure 2:** Iterate (left) and error (right) in iteration 0.

# The Parallel Schwarz Algorithm – 1D Laplace Results

Let us again consider the simple boundary value problem: Find  $u$  such that

$$-u'' = 1, \text{ in } [0, 1], \quad u(0) = u(1) = 0.$$

We perform a **parallel Schwarz iteration**:

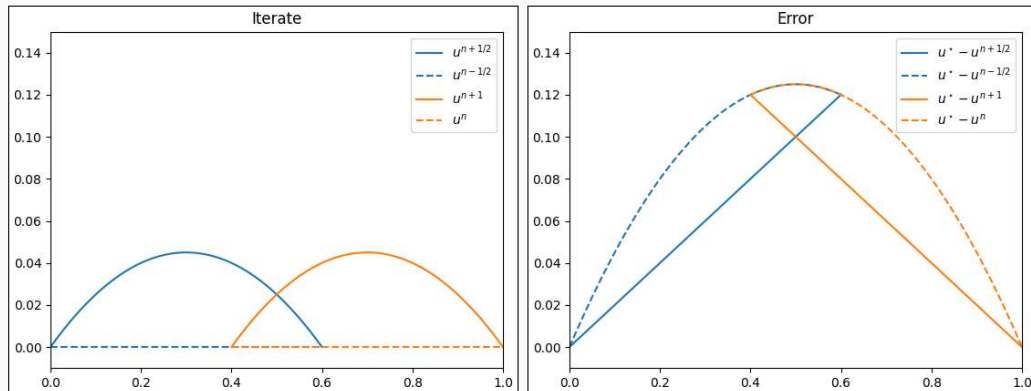


Figure 2: Iterate (left) and error (right) in iteration 1.

# The Parallel Schwarz Algorithm – 1D Laplace Results

Let us again consider the simple boundary value problem: Find  $u$  such that

$$-u'' = 1, \text{ in } [0, 1], \quad u(0) = u(1) = 0.$$

We perform a **parallel Schwarz iteration**:

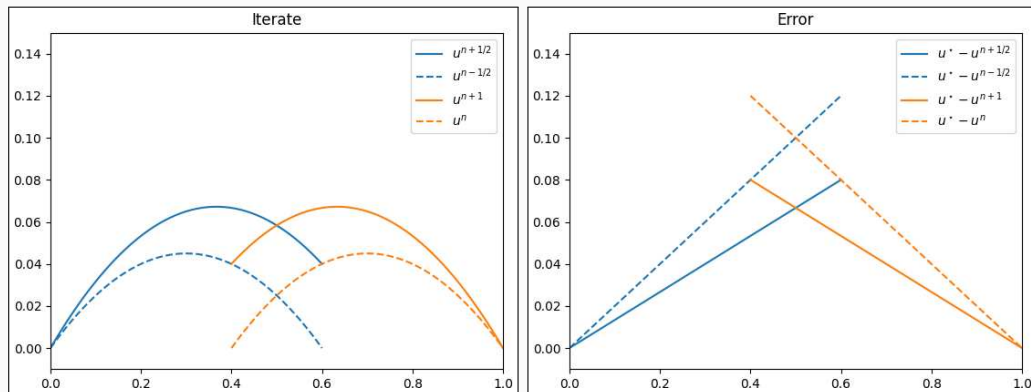


Figure 2: Iterate (left) and error (right) in iteration 2.

# The Parallel Schwarz Algorithm – 1D Laplace Results

Let us again consider the simple boundary value problem: Find  $u$  such that

$$-u'' = 1, \text{ in } [0, 1], \quad u(0) = u(1) = 0.$$

We perform a **parallel Schwarz iteration**:

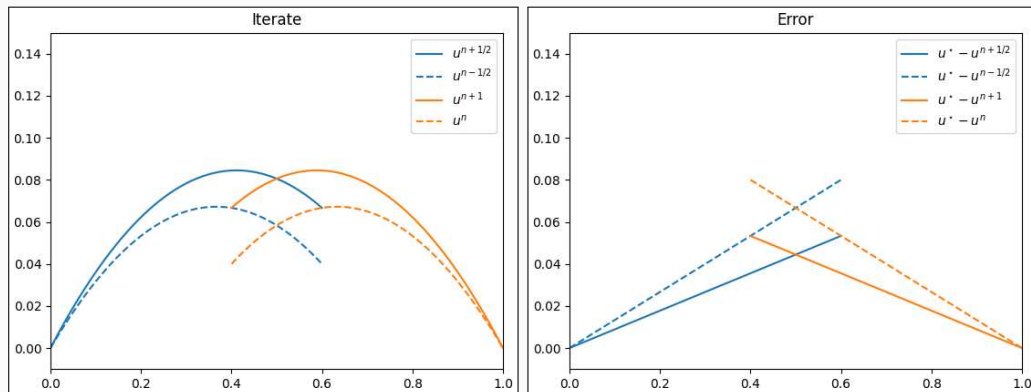


Figure 2: Iterate (left) and error (right) in iteration 3.

# The Parallel Schwarz Algorithm – 1D Laplace Results

Let us again consider the simple boundary value problem: Find  $u$  such that

$$-u'' = 1, \text{ in } [0, 1], \quad u(0) = u(1) = 0.$$

We perform a **parallel Schwarz iteration**:

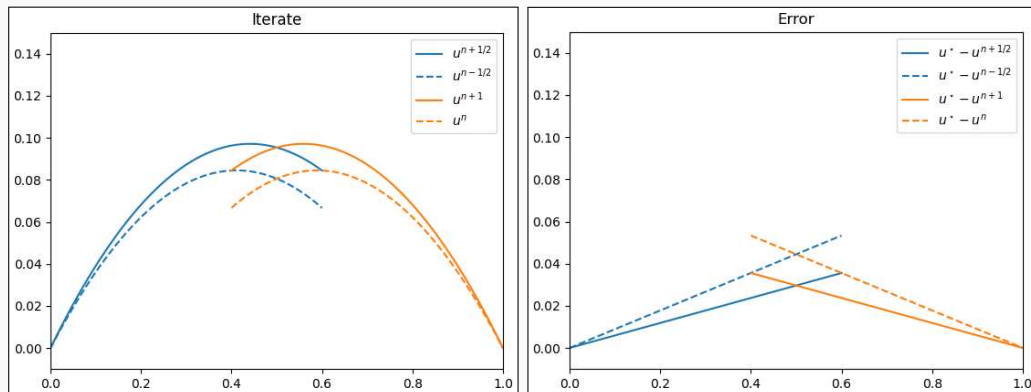


Figure 2: Iterate (left) and error (right) in iteration 4.

# The Parallel Schwarz Algorithm – 1D Laplace Results

Let us again consider the simple boundary value problem: Find  $u$  such that

$$-u'' = 1, \text{ in } [0, 1], \quad u(0) = u(1) = 0.$$

We perform a **parallel Schwarz iteration**:

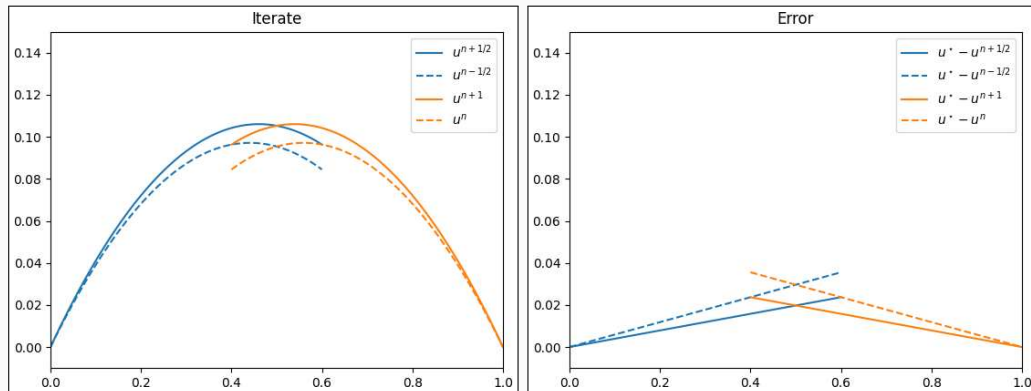
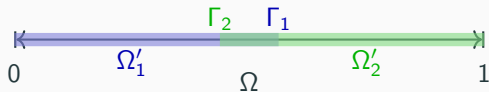


Figure 2: Iterate (left) and error (right) in iteration 5.

## Effect of the Size of the Overlap

We investigate the convergence of the methods (using the alternating method as an example) depending on the **size of the overlap**:

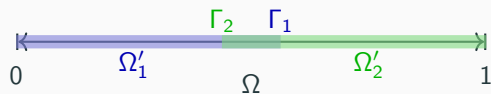


Overlap 0.05



Overlap 0.1

# Effect of the Size of the Overlap



Overlap 0.05



Overlap 0.1

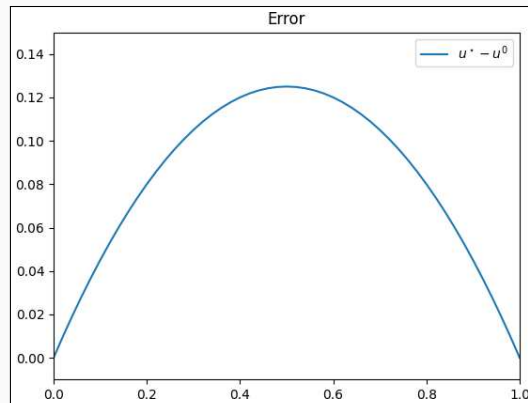
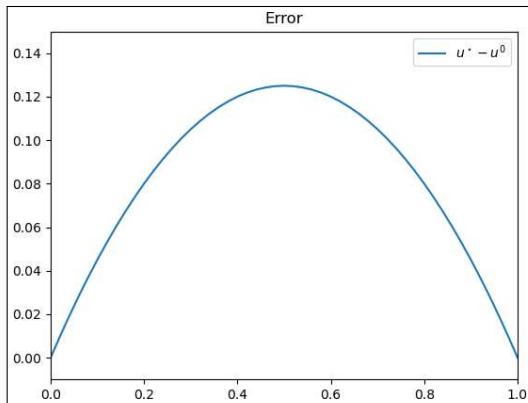
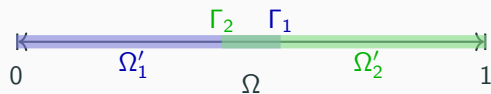


Figure 3: Error in iteration 0.

# Effect of the Size of the Overlap



Overlap 0.05



Overlap 0.1

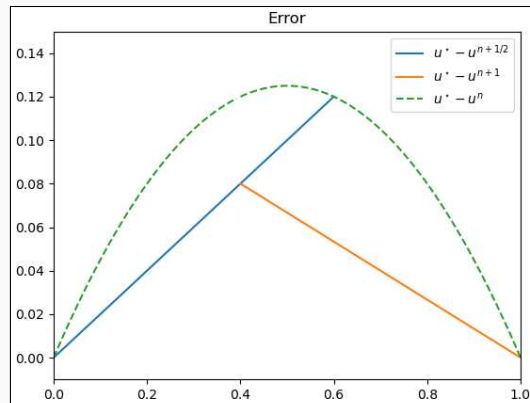
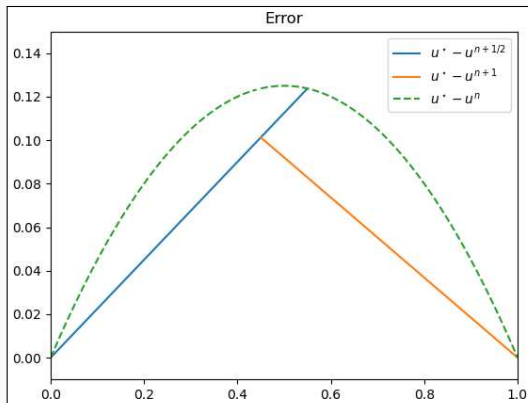
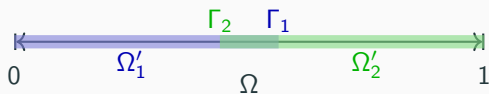


Figure 3: Error in iteration 1.

# Effect of the Size of the Overlap



Overlap 0.05



Overlap 0.1

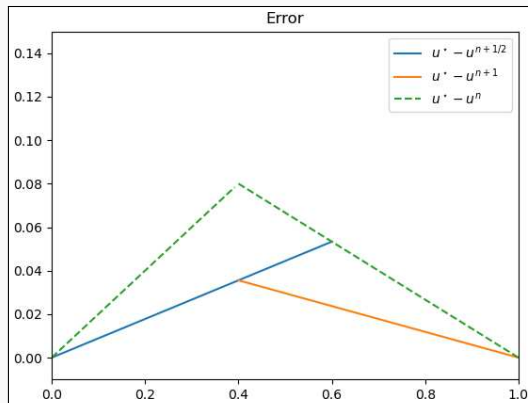
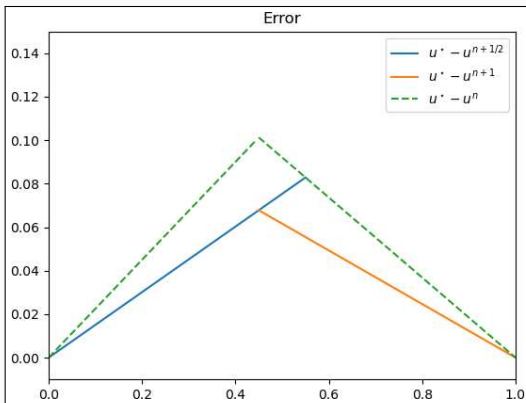
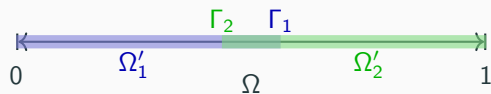


Figure 3: Error in iteration 2.

# Effect of the Size of the Overlap



Overlap 0.05



Overlap 0.1

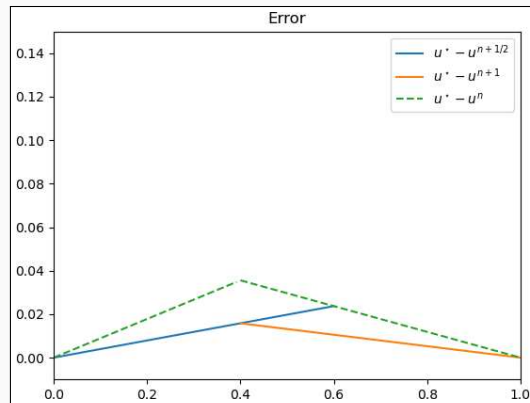
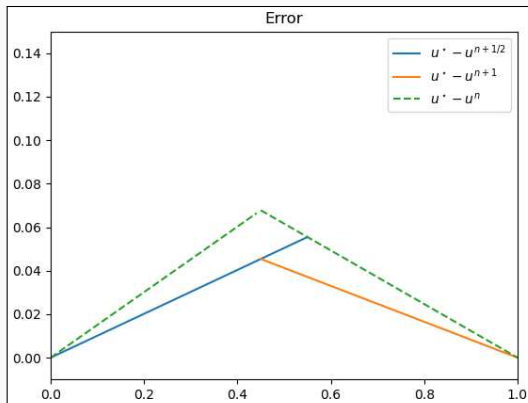
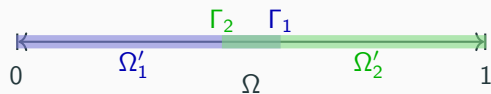


Figure 3: Error in iteration 3.

# Effect of the Size of the Overlap



Overlap 0.05



Overlap 0.1

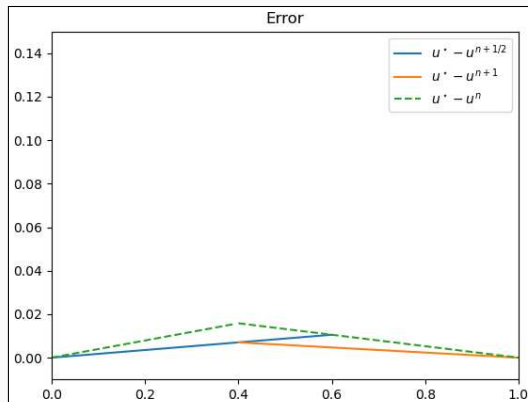
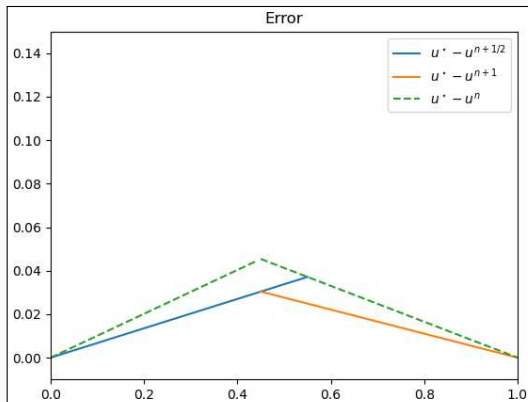
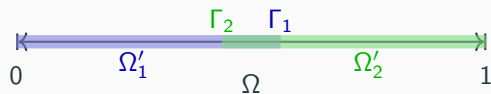


Figure 3: Error in iteration 4.

# Effect of the Size of the Overlap



Overlap 0.05



Overlap 0.1

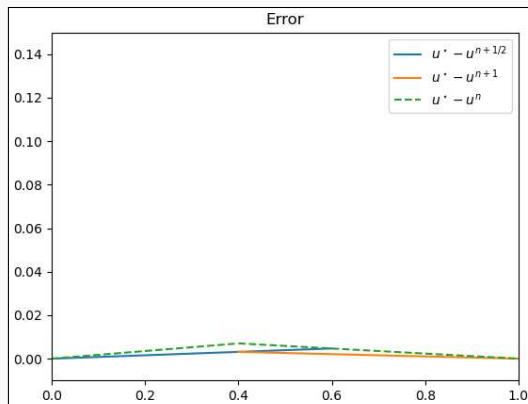
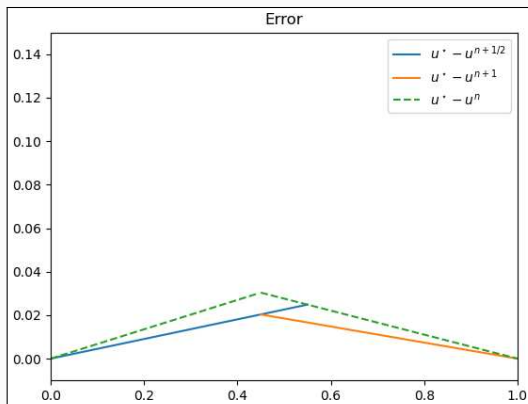
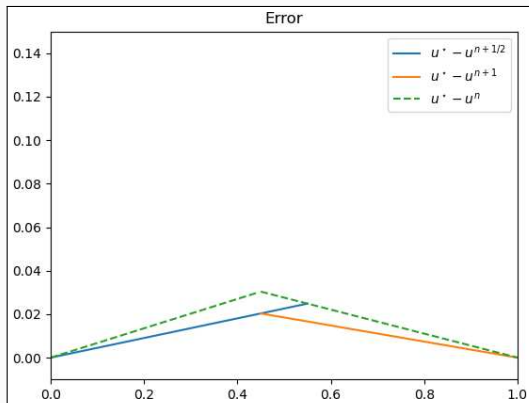


Figure 3: Error in iteration 5.

# Effect of the Size of the Overlap

## Overlap 0.05



## Overlap 0.1

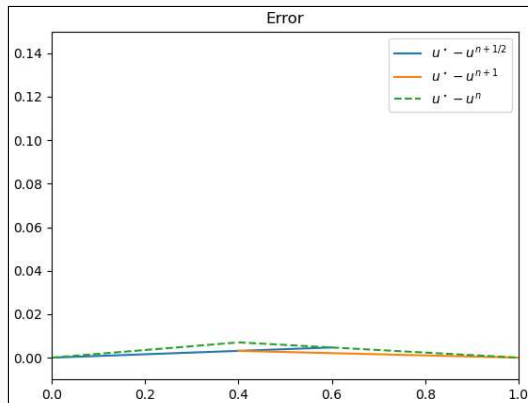


Figure 3: Error in iteration 5.

⇒ A **larger overlap** leads to **faster convergence**.

# Solvers for Partial Differential Equations

Consider a **diffusion model problem**:

$$\begin{aligned} -\Delta u(x) &= f \quad \text{in } \Omega = [0, 1]^2, \\ u &= 0 \quad \text{on } \partial\Omega. \end{aligned}$$

Discretization using finite elements yields a **sparse** system of linear equations

$$Ku = f.$$

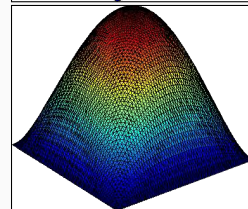
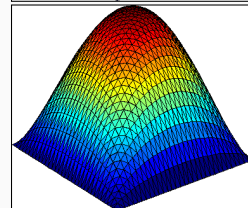
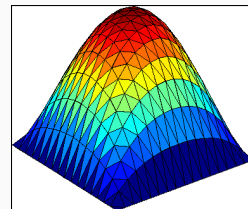
The accuracy of the finite element solution depends on the refinement level of the mesh  $h$ : **higher refinement**  $\Rightarrow$  **better accuracy**.

## Direct solvers

For fine meshes, solving the system using a direct solver is not feasible due to **superlinear complexity and memory cost**.

## Iterative solvers

**Iterative solvers are efficient** for solving **sparse systems**, however, the **convergence rate depends on the spectral properties of  $K$** .

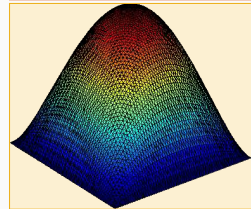
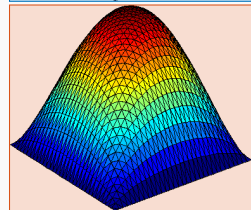
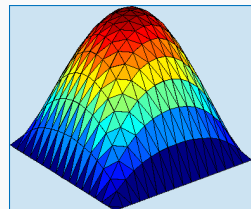
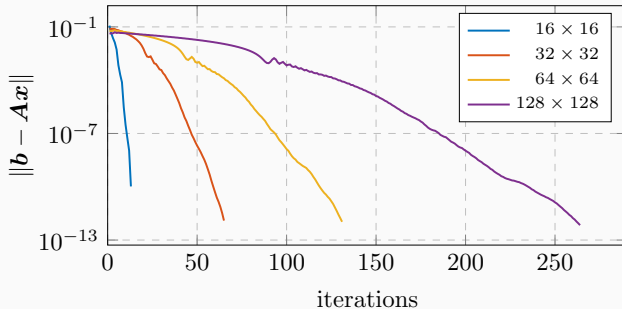


# Solvers for Partial Differential Equations

Consider a **diffusion model problem**:

$$\begin{aligned} -\Delta u(x) &= f \quad \text{in } \Omega = [0, 1]^2, \\ u &= 0 \quad \text{on } \partial\Omega. \end{aligned}$$

We solve  $Ku = f$  using the **conjugate gradient (CG) method**:

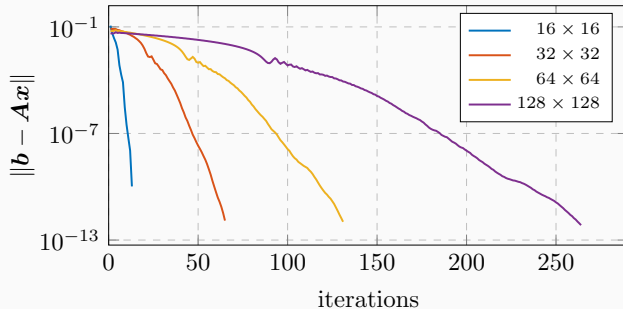


# Solvers for Partial Differential Equations

Consider a **diffusion model problem**:

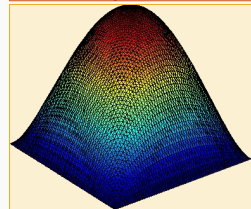
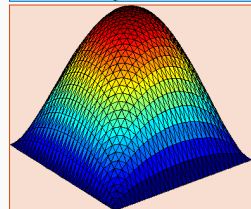
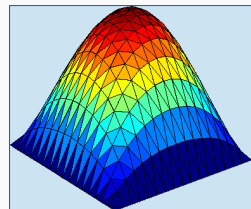
$$\begin{aligned} -\Delta u(x) &= f \quad \text{in } \Omega = [0, 1]^2, \\ u &= 0 \quad \text{on } \partial\Omega. \end{aligned}$$

We solve  $Ku = f$  using the **conjugate gradient (CG) method**:



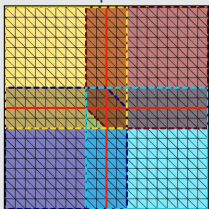
⇒ Introduce a preconditioner  $M^{-1} \approx K^{-1}$  to **improve convergence**:

$$M^{-1}Ku = M^{-1}f$$

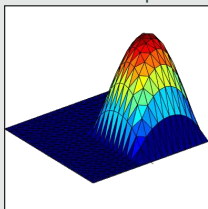


## One-level Schwarz preconditioner

Overlap  $\delta = 1h$



Solution of local problem



Based on an **overlapping domain decomposition**, we define a **one-level Schwarz operator**

$$M_{OS-1}^{-1}K = \sum_{i=1}^N R_i^\top K_i^{-1} R_i K,$$

where  $R_i$  and  $R_i^\top$  are restriction and prolongation operators corresponding to  $\Omega'_i$ , and  $K_i := R_i K R_i^\top$ .

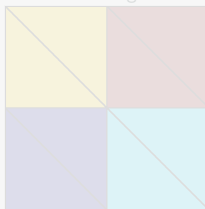
**Condition number estimate:**

$$\kappa(M_{OS-1}^{-1}K) \leq C \left(1 + \frac{1}{H\delta}\right)$$

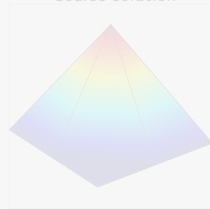
with subdomain size  $H$  and overlap width  $\delta$ .

## Lagrangian coarse space

Coarse triangulation



Coarse solution



The two-level overlapping Schwarz operator reads

$$M_{OS-2}^{-1}K = \underbrace{\Phi K_0^{-1} \Phi^\top K}_{\text{coarse level - global}} + \underbrace{\sum_{i=1}^N R_i^\top K_i^{-1} R_i K}_{\text{first level - local}}$$

where  $\Phi$  contains the coarse basis functions and  $K_0 := \Phi^\top K \Phi$ ; cf., e.g., **Toselli, Widlund (2005)**.

The construction of a Lagrangian coarse basis requires a coarse triangulation.

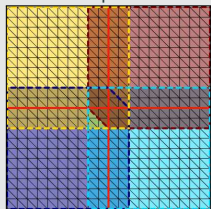
**Condition number estimate:**

$$\kappa(M_{OS-2}^{-1}K) \leq C \left(1 + \frac{H}{\delta}\right)$$

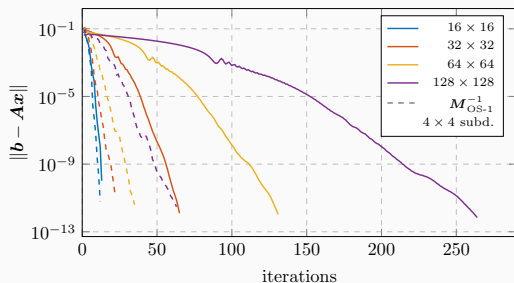
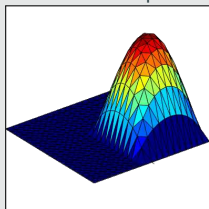
# Two-Level Schwarz Preconditioners

## One-level Schwarz preconditioner

Overlap  $\delta = 1h$

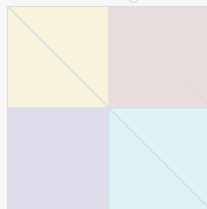


Solution of local problem



## Lagrangian coarse space

Coarse triangulation



Coarse solution



The two-level overlapping Schwarz operator reads

$$M_{OS-2}^{-1}K = \underbrace{\Phi K_0^{-1} \Phi^T K}_{\text{coarse level - global}} + \underbrace{\sum_{i=1}^N R_i^T K_i^{-1} R_i K}_{\text{first level - local}}$$

where  $\Phi$  contains the coarse basis functions and  $K_0 := \Phi^T K \Phi$ ; cf., e.g., **Toselli, Widlund (2005)**.

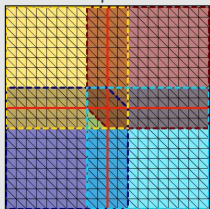
The construction of a Lagrangian coarse basis requires a coarse triangulation.

Condition number estimate:

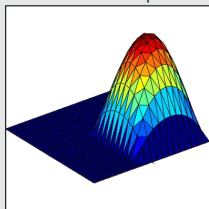
$$\kappa(M_{OS-2}^{-1}K) \leq C \left(1 + \frac{H}{\delta}\right)$$

## One-level Schwarz preconditioner

Overlap  $\delta = 1h$



Solution of local problem



Based on an **overlapping domain decomposition**, we define a **one-level Schwarz operator**

$$M_{OS-1}^{-1}K = \sum_{i=1}^N R_i^\top K_i^{-1} R_i K,$$

where  $R_i$  and  $R_i^\top$  are restriction and prolongation operators corresponding to  $\Omega'_i$ , and  $K_i := R_i K R_i^\top$ .

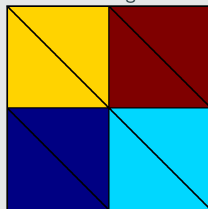
**Condition number estimate:**

$$\kappa(M_{OS-1}^{-1}K) \leq C \left(1 + \frac{1}{H\delta}\right)$$

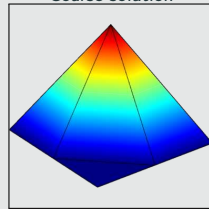
with subdomain size  $H$  and overlap width  $\delta$ .

## Lagrangian coarse space

Coarse triangulation



Coarse solution



The **two-level overlapping Schwarz operator** reads

$$M_{OS-2}^{-1}K = \underbrace{\Phi K_0^{-1} \Phi^\top K}_{\text{coarse level - global}} + \underbrace{\sum_{i=1}^N R_i^\top K_i^{-1} R_i K}_{\text{first level - local}}$$

where  $\Phi$  contains the coarse basis functions and  $K_0 := \Phi^\top K \Phi$ ; cf., e.g., **Toselli, Widlund (2005)**.

The construction of a Lagrangian coarse basis requires a coarse triangulation.

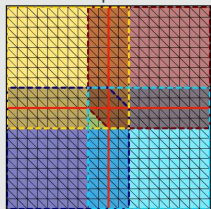
**Condition number estimate:**

$$\kappa(M_{OS-2}^{-1}K) \leq C \left(1 + \frac{H}{\delta}\right)$$

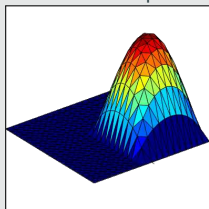
# Two-Level Schwarz Preconditioners

## One-level Schwarz preconditioner

Overlap  $\delta = 1h$

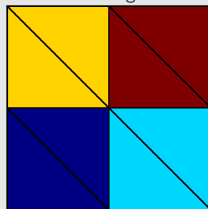


Solution of local problem

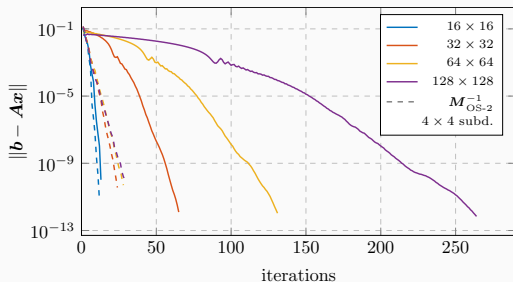
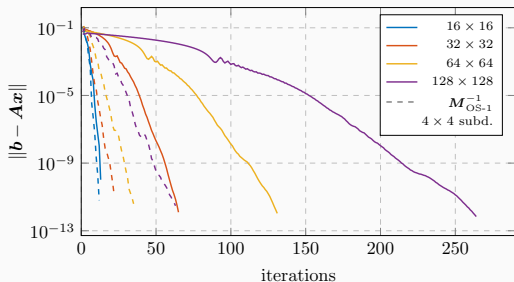
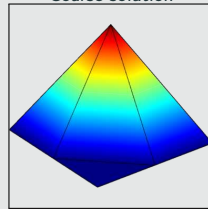


## Lagrangian coarse space

Coarse triangulation



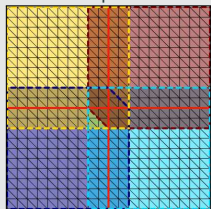
Coarse solution



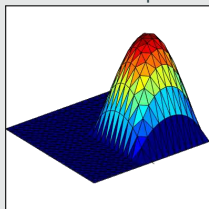
# Two-Level Schwarz Preconditioners

## One-level Schwarz preconditioner

Overlap  $\delta = 1h$

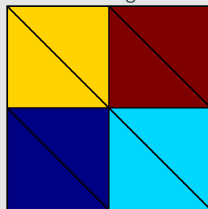


Solution of local problem

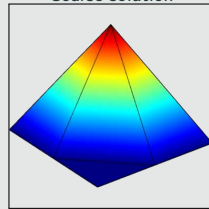


## Lagrangian coarse space

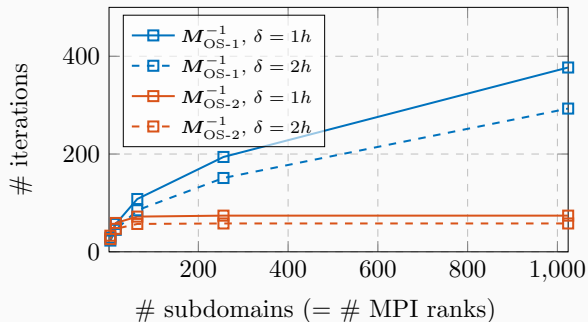
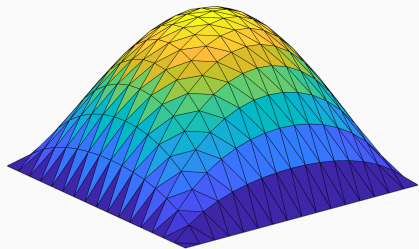
Coarse triangulation



Coarse solution



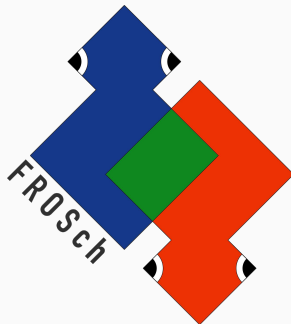
Diffusion model problem in two dimensions,  
 $H/h = 100$



# **The FROSch Package – Algebraic and Parallel Schwarz Preconditioners in Trilinos**

---

# FROSch (Fast and Robust Overlapping Schwarz) Framework in Trilinos



Sandia  
National  
Laboratories



TUBAF  
Die Ressourcenuniversität.  
Seit 1765.

## Software

- Object-oriented C++ domain decomposition solver framework with MPI-based distributed memory parallelization
- Part of TRILINOS with support for both parallel linear algebra packages EPETRA and TPETRA
- Node-level parallelization and performance portability on CPU and GPU architectures through KOKKOS and KOKKOSKERNELS
- Accessible through unified TRILINOS solver interface STRATIMIKOS

## Methodology

- **Parallel scalable multi-level Schwarz domain decomposition preconditioners**
- **Algebraic construction** based on the parallel distributed system matrix
- **Extension-based coarse spaces**

## Team (active)

- Filipe Cumaru (TU Delft)
- Kyrill Ho (UCologne)
- Jascha Knepper (UCologne)
- Friederike Röver (TUBAF)
- Lea Saßmannshausen (UCologne)
- Alexander Heinlein (TU Delft)
- Axel Klawonn (UCologne)
- Siva Rajamanickam (SNL)
- Oliver Rheinbach (TUBAF)
- Ichitaro Yamazaki (SNL)

# Partition of Unity

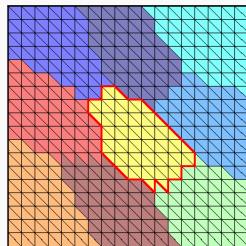
The **energy-minimizing extension**  $v_i = H_{\partial\Omega_i \rightarrow \Omega_i}(v_{i, \partial\Omega_i})$  solves

$$\begin{aligned} -\Delta v_i &= 0 && \text{in } \Omega_i, \\ v_i &= v_{i, \partial\Omega_i} && \text{on } \partial\Omega_i. \end{aligned}$$

Hence,  $v_i = E_{\partial\Omega_i \rightarrow \Omega_i}(\mathbb{1}_{\partial\Omega_i}) = \mathbb{1}$ .

Due to **linearity of the extension operator**, we have

$$\sum_i \varphi_i = \mathbb{1}_{\partial\Omega_i} \Rightarrow \sum_i E_{\partial\Omega_i \rightarrow \Omega_i}(\varphi_i) = \mathbb{1}_{\Omega_i}$$



## Null space property

Any extension-based coarse space built from a partition of unity on the domain decomposition interface satisfies the **null space property necessary for numerical scalability**:



## Algebraicity of the energy-minimizing extension

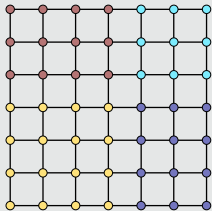
The computation of energy-minimizing extensions only requires  $K_{II}$  and  $K_{I\Gamma}$ , **submatrices of the fully assembled matrix  $K_i$** .

$$\mathbf{v} = \begin{bmatrix} -K_{II}^{-1} K_{I\Gamma} \\ I_{\Gamma} \end{bmatrix} \mathbf{v}_{\Gamma},$$

# FROSch Construction – Graph View

In the algebraic construction of FROSch preconditioners, we use **two different graphs**:

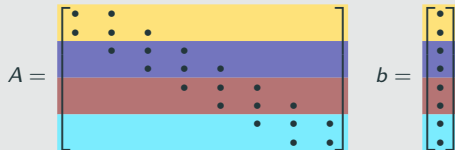
## Node graph



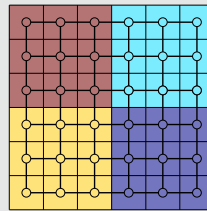
The **node graph** coincides with the simulation mesh of the computational domain:

- Graph nodes  $\equiv$  mesh nodes
- Graph edges  $\equiv$  mesh element edges

In parallel simulations:



## Dual graph



The **dual graph** represents the connectivity of mesh elements:

- Graph nodes  $\equiv$  mesh elements
- Graph edges  $\equiv$  shared edges between mesh elements

In parallel finite element simulations, where the matrix assembly is element-based, the **distribution of the data** is done based on a partition of the dual graph.

## Overlapping domain decomposition

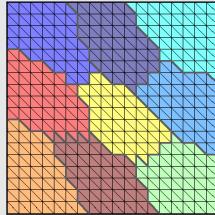
The **overlapping subdomains** are constructed by **recursively adding layers of elements**.

The corresponding matrices

$$K_i = R_i K R_i^T$$

can easily be extracted from  $K$ .

### Nonoverlapping DD



## Overlapping domain decomposition

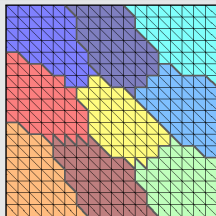
The **overlapping subdomains** are constructed by **recursively adding layers of elements**.

The corresponding matrices

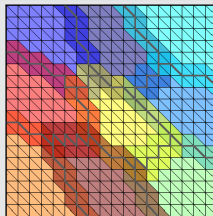
$$K_i = R_i K R_i^T$$

can easily be extracted from  $K$ .

Nonoverlapping DD



Overlap  $\delta = 1h$



## Overlapping domain decomposition

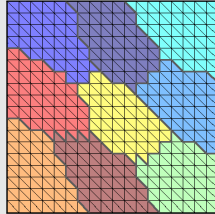
The **overlapping subdomains** are constructed by **recursively adding layers of elements**.

The corresponding matrices

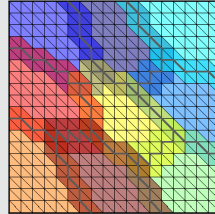
$$K_i = R_i K R_i^T$$

can easily be extracted from  $K$ .

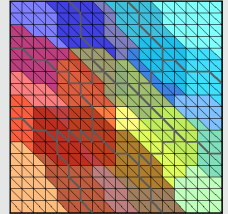
Nonoverlapping DD



Overlap  $\delta = 1h$



Overlap  $\delta = 2h$



## Overlapping domain decomposition

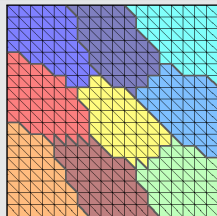
The **overlapping subdomains** are constructed by **recursively adding layers of elements**.

The corresponding matrices

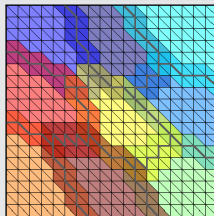
$$K_i = R_i K R_i^T$$

can easily be extracted from  $K$ .

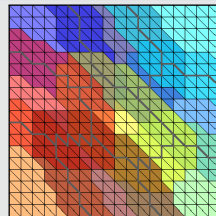
Nonoverlapping DD



Overlap  $\delta = 1h$

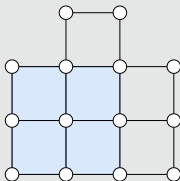


Overlap  $\delta = 2h$



## Implementation as a graph search problem

The overlapping subdomains can be seen as the result of a limited **breadth first search** on the graph representing the sparsity pattern of  $K$ .



## Overlapping domain decomposition

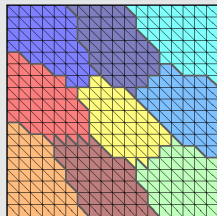
The **overlapping subdomains** are constructed by **recursively adding layers of elements**.

The corresponding matrices

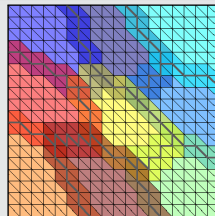
$$K_i = R_i K R_i^T$$

can easily be extracted from  $K$ .

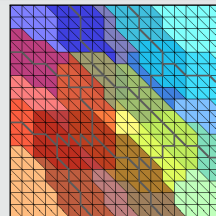
Nonoverlapping DD



Overlap  $\delta = 1h$

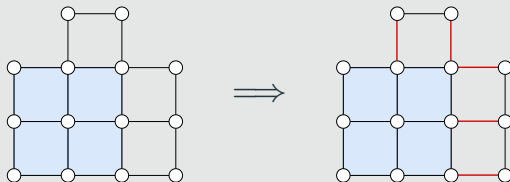


Overlap  $\delta = 2h$



## Implementation as a graph search problem

The overlapping subdomains can be seen as the result of a limited **breadth first search** on the graph representing the sparsity pattern of  $K$ .



## Overlapping domain decomposition

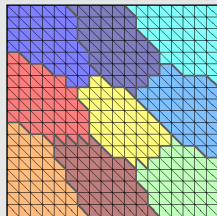
The **overlapping subdomains** are constructed by **recursively adding layers of elements**.

The corresponding matrices

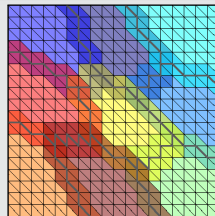
$$K_i = R_i K R_i^T$$

can easily be extracted from  $K$ .

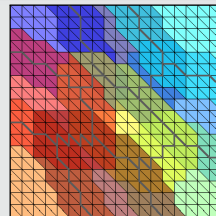
Nonoverlapping DD



Overlap  $\delta = 1h$

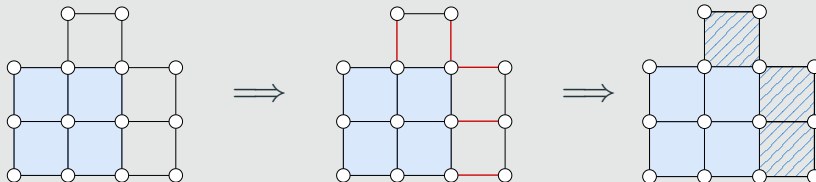


Overlap  $\delta = 2h$



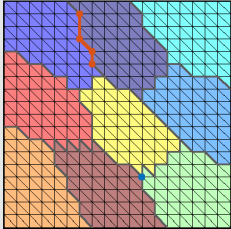
## Implementation as a graph search problem

The overlapping subdomains can be seen as the result of a limited **breadth first search** on the graph representing the sparsity pattern of  $K$ .



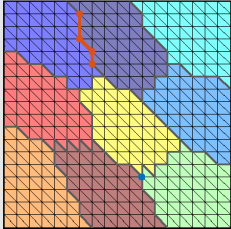
## Coarse space

### 1. Interface components

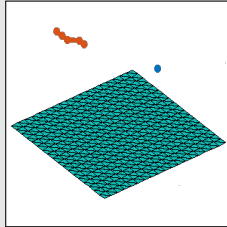


## Coarse space

### 1. Interface components



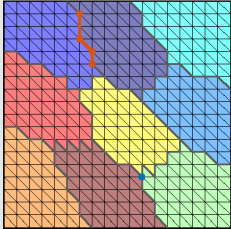
### 2. Interface basis (partition of unity $\times$ null space)



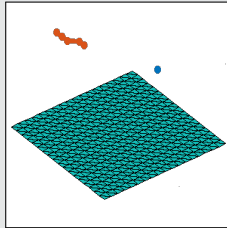
For **scalar elliptic problems**, the **null space** consists only of **constant functions**.

## Coarse space

### 1. Interface components

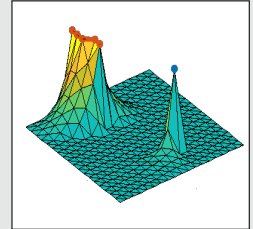


### 2. Interface basis (partition of unity $\times$ null space)



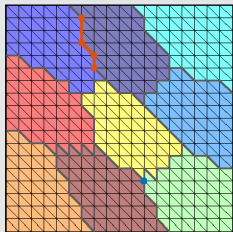
For scalar elliptic problems, the null space consists only of constant functions.

### 3. Extension

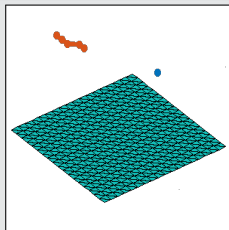


## Coarse space

### 1. Interface components

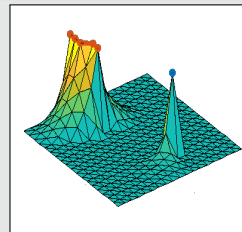


### 2. Interface basis (partition of unity $\times$ null space)



For scalar elliptic problems, the null space consists only of constant functions.

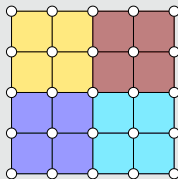
### 3. Extension



## Construction of the interface entities

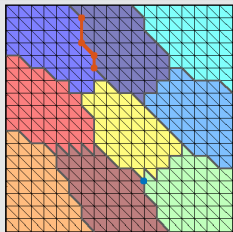
A partition of interface entities can be found by inspecting the dual graph of the mesh.

If it is **not given as an input**, it **can generally not be retained** from the sparsity pattern of  $K$ , but we can approximate it.

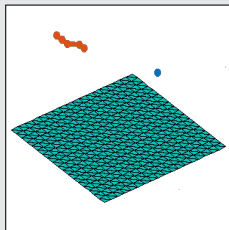


## Coarse space

### 1. Interface components

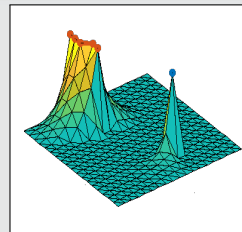


### 2. Interface basis (partition of unity $\times$ null space)



For scalar elliptic problems, the null space consists only of constant functions.

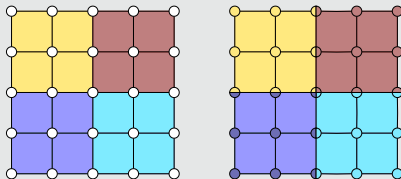
### 3. Extension



## Construction of the interface entities

A partition of interface entities can be found by inspecting the dual graph of the mesh.

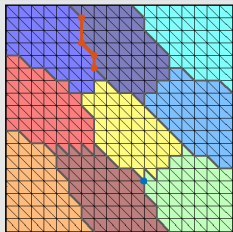
If it is **not given as an input**, it **can generally not be retained** from the sparsity pattern of  $K$ , but we can approximate it.



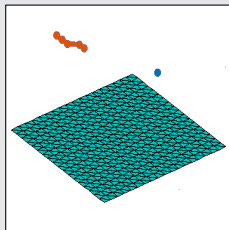
# Algorithmic Framework for FROSch Preconditioners

## Coarse space

### 1. Interface components

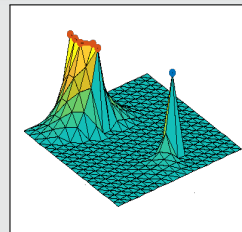


### 2. Interface basis (partition of unity $\times$ null space)



For scalar elliptic problems, the null space consists only of constant functions.

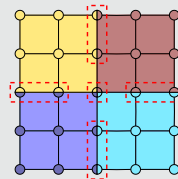
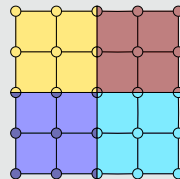
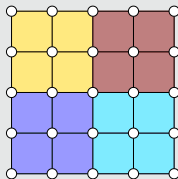
### 3. Extension



## Construction of the interface entities

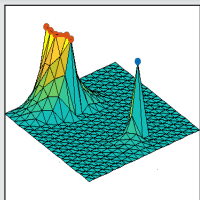
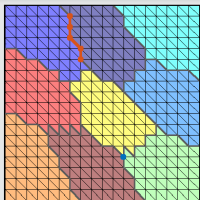
A partition of interface entities can be found by inspecting the dual graph of the mesh.

If it is **not given as an input**, it **can generally not be retained** from the sparsity pattern of  $K$ , but we can approximate it.



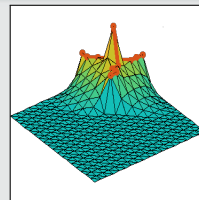
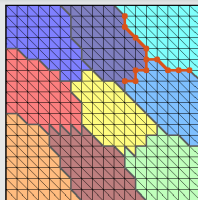
# Examples of FROSch Coarse Spaces

## GDSW (Generalized Dryja–Smith–Widlund)



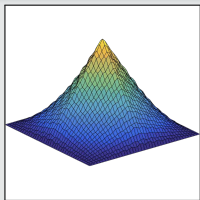
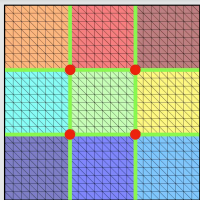
- Dohrmann, Klawonn, Widlund (2008)
- Dohrmann, Widlund (2009, 2010, 2012)

## RGDSW (Reduced dimension GDSW)



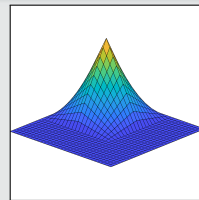
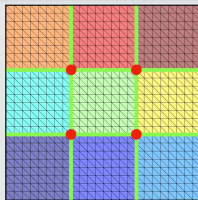
- Dohrmann, Widlund (2017)
- H., Klawonn, Knepper, Rheinbach, Widlund (2022)

## MsFEM (Multiscale Finite Element Method)



- Hou (1997), Efendiev and Hou (2009)
- Buck, Iliev, and Andrä (2013)
- H., Klawonn, Knepper, Rheinbach (2018)

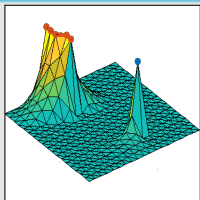
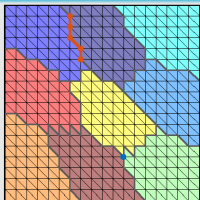
## Q1 Lagrangian / piecewise bilinear



Piecewise linear interface partition of unity functions and a structured domain decomposition.

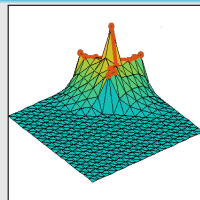
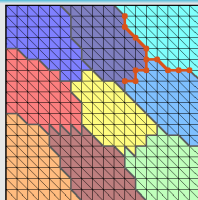
# Examples of FROSch Coarse Spaces

## GDSW (Generalized Dryja–Smith–Widlund)



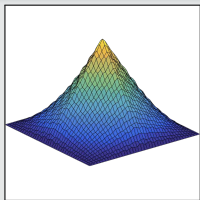
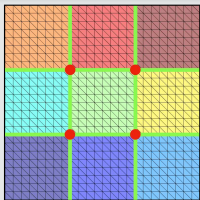
- Dohrmann, Klawonn, Widlund (2008)
- Dohrmann, Widlund (2009, 2010, 2012)

## RGDSW (Reduced dimension GDSW)



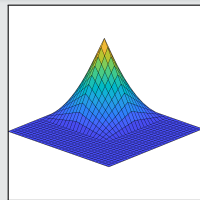
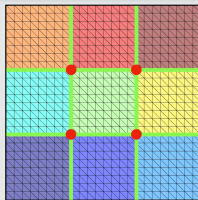
- Dohrmann, Widlund (2017)
- H., Klawonn, Knepper, Rheinbach, Widlund (2022)

## MsFEM (Multiscale Finite Element Method)



- Hou (1997), Efendiev and Hou (2009)
- Buck, Iliev, and Andrä (2013)
- H., Klawonn, Knepper, Rheinbach (2018)

## Q1 Lagrangian / piecewise bilinear

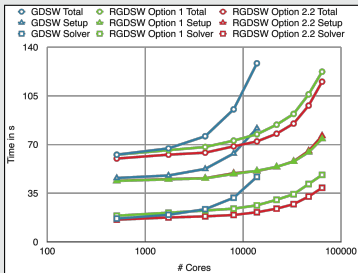
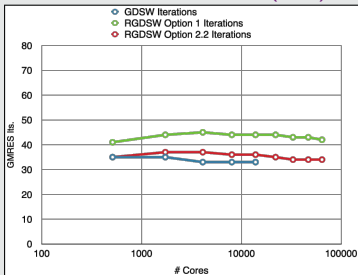


Piecewise linear interface partition of unity functions and a structured domain decomposition.

# Weak Scalability up to 64k MPI Ranks / 1.7b Unknowns (3D Poisson; Juqueen)

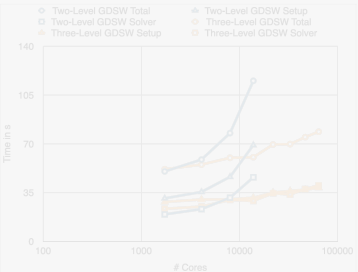
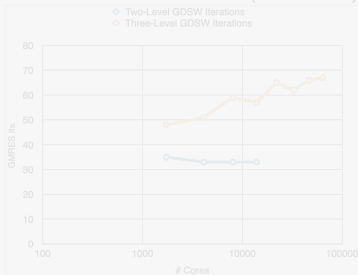
## GDSW vs RGDSW (reduced dimension)

Heinlein, Klawonn, Rheinbach, Widlund (2019).



## Two-level vs three-level GDSW

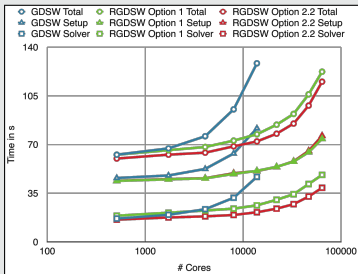
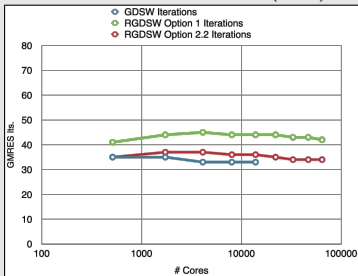
Heinlein, Klawonn, Rheinbach, Röver (2019, 2020).



# Weak Scalability up to 64k MPI Ranks / 1.7b Unknowns (3D Poisson; Juqueen)

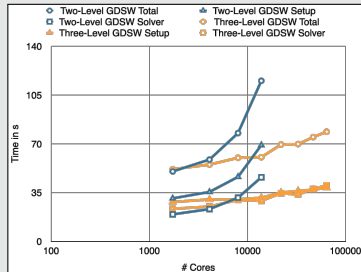
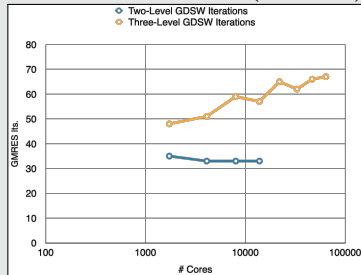
## GDSW vs RGDSW (reduced dimension)

Heinlein, Klawonn, Rheinbach, Widlund (2019).



## Two-level vs three-level GDSW

Heinlein, Klawonn, Rheinbach, Röver (2019, 2020).



## **Some Challenging Application Problems**

---

# Monolithic (R)GDSW Preconditioners for CFD Simulations

Consider the discrete saddle point problem

$$\mathcal{A}x = \begin{bmatrix} \mathbf{K} & \mathbf{B}^\top \\ \mathbf{B} & \mathbf{0} \end{bmatrix} \begin{bmatrix} \mathbf{u} \\ \mathbf{p} \end{bmatrix} = \begin{bmatrix} \mathbf{f} \\ \mathbf{0} \end{bmatrix} = \mathbf{b}.$$

## Monolithic GDSW preconditioner

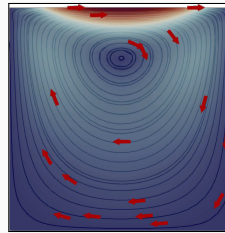
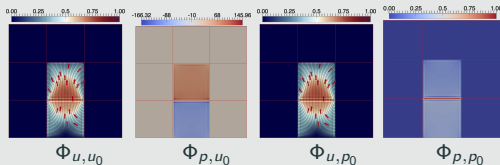
We construct a **monolithic GDSW preconditioner**

$$m_{\text{GDSW}}^{-1} = \phi \mathcal{A}_0^{-1} \phi^\top + \sum_{i=1}^N \mathcal{R}_i^\top \bar{\mathcal{P}}_i \mathcal{A}_i^{-1} \mathcal{R}_i,$$

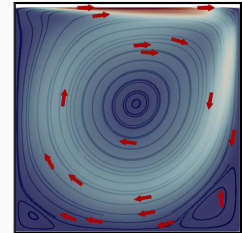
with block matrices  $\mathcal{A}_0 = \phi^\top \mathcal{A} \phi$ ,  $\mathcal{A}_i = \mathcal{R}_i \mathcal{A} \mathcal{R}_i^\top$ , local pressure projections  $\bar{\mathcal{P}}_i$ , and

$$\mathcal{R}_i = \begin{bmatrix} \mathcal{R}_{u,i} & \mathbf{0} \\ \mathbf{0} & \mathcal{R}_{p,i} \end{bmatrix} \quad \text{and} \quad \phi = \begin{bmatrix} \Phi_{u,u_0} & \Phi_{u,p_0} \\ \Phi_{p,u_0} & \Phi_{p,p_0} \end{bmatrix}.$$

Using  $\mathcal{A}$  to compute extensions:  $\phi_l = -\mathcal{A}_{ll}^{-1} \mathcal{A}_{ll} \phi_l$ ; cf. **Heinlein, Hochmuth, Klawonn (2019, 2020)**.



Stokes flow



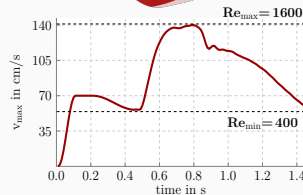
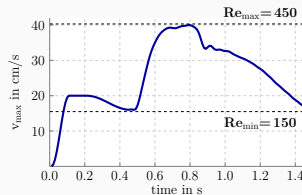
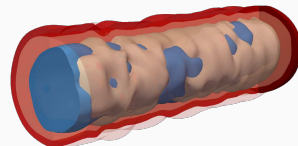
Navier–Stokes flow

## Related work:

- Original work on monolithic Schwarz preconditioners: **Klawonn and Pavarino (1998, 2000)**
- Other publications on monolithic Schwarz preconditioners: e.g., **Hwang and Cai (2006)**, **Barker and Cai (2010)**, **Wu and Cai (2014)**, and the presentation **Dohrmann (2010)** at the *Workshop on Adaptive Finite Elements and Domain Decomposition Methods in Milan*.

# Results for Blood Flow Simulations

- **3D unsteady flow simulation** within the **geometry of a realistic artery** (from **Balzani et al. (2012)**) and kinematic viscosity  $\nu = 0.03 \text{ cm}^2/\text{s}$
- **Parabolic inflow profile** is prescribed at inlet of geometry
- **Time discretization:** BDF-2; **space discretization:** P2-P1 elements



prec.	# MPI ranks	16	64	256
Monolithic RGDSW (FRO <sub>SCH</sub> )	avg. #its.	33	31	30
	setup	4 825 s	1 422 s	701 s
	solve	3 198 s	1 004 s	463 s
	total	8 023 s	2 426 s	<b>1 164 s</b>
SIMPLE RGDSW (TE <sub>KO</sub> & FRO <sub>SCH</sub> )	avg. #its.	82	82	87
	setup	3 046 s	824 s	428 s
	solve	4 679 s	1 533 s	801 s
	total	<b>7 725 s</b>	<b>2 357 s</b>	1 229 s

prec.	# MPI ranks	16	64	256
Monolithic RGDSW (FRO <sub>SCH</sub> )	avg. #its.	36	36	36
	setup	4 808 s	1 448 s	688 s
	solve	3 490 s	1 186 s	538 s
	total	<b>8 298 s</b>	<b>2 634 s</b>	<b>1 226 s</b>
SIMPLE RGDSW (TE <sub>KO</sub> & FRO <sub>SCH</sub> )	avg. #its.	157	164	169
	setup	3 071 s	842 s	432 s
	solve	9 541 s	3 210 s	1 585 s
	total	12 612 s	4 052 s	2 017 s

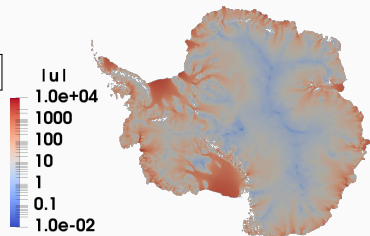


<https://github.com/SNLComputation/Albany>

The velocity of the ice sheet in Antarctica and Greenland is modeled by a **first-order-accurate Stokes approximation model**,

$$-\nabla \cdot (2\mu\dot{\epsilon}_1) + \rho g \frac{\partial s}{\partial x} = 0, \quad -\nabla \cdot (2\mu\dot{\epsilon}_2) + \rho g \frac{\partial s}{\partial y} = 0,$$

with a **nonlinear viscosity model** (Glen's law); cf., e.g., **Blatter (1995)** and **Pattyn (2003)**.



MPI ranks	Antarctica ( <b>velocity</b> )			Greenland ( <b>multiphysics vel. &amp; temperature</b> )		
	4 km resolution, 20 layers, 35 m dofs			1-10 km resolution, 20 layers, 69 m dofs		
	avg. its	avg. setup	avg. solve	avg. its	avg. setup	avg. solve
512	<b>41.9</b> (11)	25.10 s	12.29 s	<b>41.3</b> (36)	18.78 s	4.99 s
1 024	<b>43.3</b> (11)	9.18 s	5.85 s	<b>53.0</b> (29)	8.68 s	4.22 s
2 048	<b>41.4</b> (11)	4.15 s	2.63 s	<b>62.2</b> (86)	4.47 s	4.23 s
4 096	<b>41.2</b> (11)	1.66 s	1.49 s	<b>68.9</b> (40)	2.52 s	2.86 s
8 192	<b>40.2</b> (11)	1.26 s	1.06 s	-	-	-

Computations performed on Cori (NERSC).

**Heinlein, Perego, Rajamanickam (2022)**

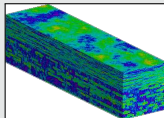
# Spectral Extension-Based Coarse Spaces for Schwarz Preconditioners

## Highly heterogeneous problems ...

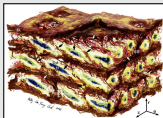
... appear in most areas of modern science and engineering:



Micro section of a dual-phase steel.  
Courtesy of **J. Schröder**.



Groundwater flow (SPE10);  
cf. **Christie and Blunt (2001)**.



Composition of arterial walls; taken from **O'Connell et al. (2008)**.

## Spectral coarse spaces

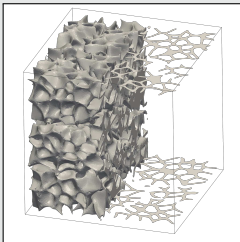
The coarse space is **enhanced** by eigenfunctions of **local edge and face eigenvalue problems** with eigenvalues below tolerances  $tol_{\mathcal{E}}$  and  $tol_{\mathcal{F}}$ :

$$\kappa(M_*^{-1}K) \leq C \left( 1 + \frac{1}{tol_{\mathcal{E}}} + \frac{1}{tol_{\mathcal{F}}} + \frac{1}{tol_{\mathcal{E}} \cdot tol_{\mathcal{F}}} \right);$$

$C$  does not depend on  $h$ ,  $H$ , or the coefficients.

**OS-ACMS** & **adaptive GDSW (AGDSW)** (**Heinlein, Klawonn, Knepper, Rheinbach (2018, 2018, 2019)**).

## Foam coefficient function example



**Solid phase:**  $\alpha = 10^6$ ; **transparent phase:**  $\alpha = 1$ ; 100 subdomains

$V_0$	$tol_{\mathcal{E}}$	$tol_{\mathcal{F}}$	it.	$\kappa$	dim $V_0$	dim $V_0$ / dof
$V_{\text{GDSW}}$	—	—	<b>565</b>	<b><math>1.3 \cdot 10^6</math></b>	1601	0.27 %
$V_{\text{AGDSW}}$	0.05	0.05	<b>60</b>	<b>30.2</b>	1968	0.33 %
$V_{\text{OS-ACMS}}$	0.001	0.001	<b>57</b>	<b>30.3</b>	690	0.12 %

Cf. **Heinlein, Klawonn, Knepper, Rheinbach (2018, 2019)**.

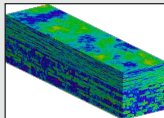
# Spectral Extension-Based Coarse Spaces for Schwarz Preconditioners

## Highly heterogeneous problems ...

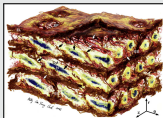
... appear in most areas of modern science and engineering:



Micro section of a dual-phase steel.  
Courtesy of **J. Schröder**.



Groundwater flow (SPE10);  
cf. **Christie and Blunt (2001)**.



Composition of arterial walls; taken from **O'Connell et al. (2008)**.

## Spectral coarse spaces

The coarse space is **enhanced** by eigenfunctions of **local edge and face eigenvalue problems** with eigenvalues below tolerances  $tol_{\mathcal{E}}$  and  $tol_{\mathcal{F}}$ :

$$\kappa(M_*^{-1}K) \leq C \left( 1 + \frac{1}{tol_{\mathcal{E}}} + \frac{1}{tol_{\mathcal{F}}} + \frac{1}{tol_{\mathcal{E}} \cdot tol_{\mathcal{F}}} \right);$$

$C$  does not depend on  $h$ ,  $H$ , or the coefficients.

**OS-ACMS & adaptive GDSW (AGDSW)** (**Heinlein, Klawonn, Knepper, Rheinbach (2018, 2018, 2019)**).

## Local eigenvalue problems

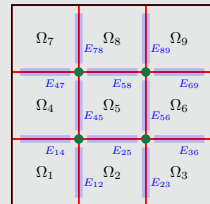
Local generalized eigenvalue problems corresponding to the edges  $\mathcal{E}$  and faces  $\mathcal{F}$  of the domain decomposition:

$$\forall E \in \mathcal{E}: \quad S_{EE}T_{*,E} = \lambda_{*,E} K_{EE}T_{*,E}, \quad \forall T_{*,E} \in V_E,$$

$$\forall F \in \mathcal{F}: \quad S_{FF}T_{*,F} = \lambda_{*,F} K_{FF}T_{*,F}, \quad \forall T_{*,F} \in V_F,$$

with **Schur complements**  $S_{EE}$ ,  $S_{FF}$  with **Neumann boundary conditions** and **submatrices**  $K_{EE}$ ,  $K_{FF}$  of  $K$ . We select eigenfunctions corresponding to **eigenvalues below tolerances**  $tol_{\mathcal{E}}$  and  $tol_{\mathcal{F}}$ .

→ The corresponding coarse basis functions are **energy-minimizing extensions** into the interior of the subdomains.



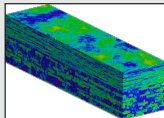
# Spectral Extension-Based Coarse Spaces for Schwarz Preconditioners

## Highly heterogeneous problems ...

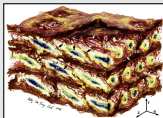
... appear in most areas of modern science and engineering:



Micro section of a dual-phase steel.  
Courtesy of **J. Schröder**.



Groundwater flow (SPE10);  
cf. **Christie and Blunt (2001)**.



Composition of arterial walls; taken from **O'Connell et al. (2008)**.

## Spectral coarse spaces

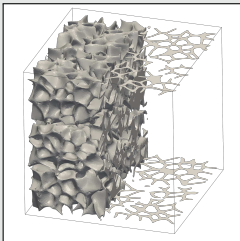
The coarse space is **enhanced** by eigenfunctions of **local edge and face eigenvalue problems** with eigenvalues below tolerances  $tol_{\mathcal{E}}$  and  $tol_{\mathcal{F}}$ :

$$\kappa(M_*^{-1}K) \leq C \left( 1 + \frac{1}{tol_{\mathcal{E}}} + \frac{1}{tol_{\mathcal{F}}} + \frac{1}{tol_{\mathcal{E}} \cdot tol_{\mathcal{F}}} \right);$$

$C$  does not depend on  $h$ ,  $H$ , or the coefficients.

**OS-ACMS** & **adaptive GDSW (AGDSW)** (**Heinlein, Klawonn, Knepper, Rheinbach (2018, 2018, 2019)**).

## Foam coefficient function example



**Solid phase:**  $\alpha = 10^6$ ; **transparent phase:**  $\alpha = 1$ ; 100 subdomains

$V_0$	$tol_{\mathcal{E}}$	$tol_{\mathcal{F}}$	it.	$\kappa$	dim $V_0$	dim $V_0$ / dof
$V_{\text{GDSW}}$	—	—	<b>565</b>	<b><math>1.3 \cdot 10^6</math></b>	1601	0.27 %
$V_{\text{AGDSW}}$	0.05	0.05	<b>60</b>	<b>30.2</b>	1968	0.33 %
$V_{\text{OS-ACMS}}$	0.001	0.001	<b>57</b>	<b>30.3</b>	690	0.12 %

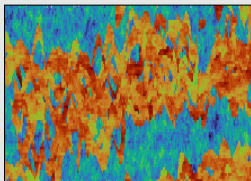
Cf. **Heinlein, Klawonn, Knepper, Rheinbach (2018, 2019)**.

# Domain Decomposition for Reservoir Simulations

## Algebraic multiscale coarse space

- We investigate **scalable and robust** simulation methods for underground hydrogen storage.
- We consider **two-level domain decomposition solver with algebraic multiscale solver (AMS)** coarse space; cf. **Wang, Hajibeygi and Tchelepi (2014)**.

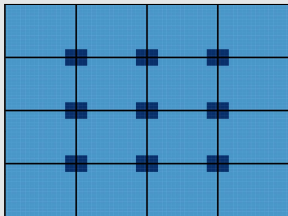
## Numerical results - SPE10 benchmark



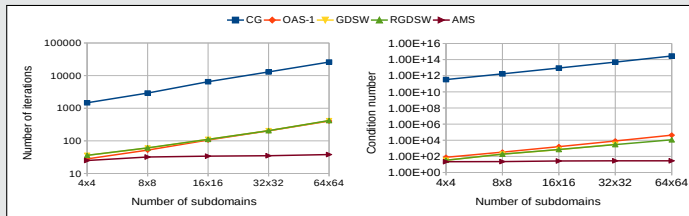
Layer 72 from model 2; cf. **Christie and Blunt (2001)**.

preconditioner	its.	$\kappa$
-	$> 10^4$	$8.61 \cdot 10^8$
one-level	174	$1.01 \cdot 10^5$
two-level w\ AMS	78	144.33

## Numerical results - Weak scalability for high coefficient inclusions



Dark blue:  $\alpha = 10^8$ ; light blue:  $\alpha = 1$



Cf. **Alves, Heinlein and Hajibeygi (2024; preprint arXiv)**

# Learning Extension Operators Using Graph Neural Networks

---

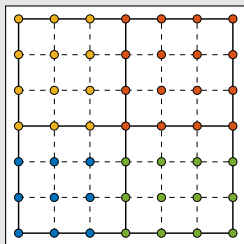
# Learning Extension Operators

Most coarse spaces for Schwarz preconditioners are constructed based on a **characteristic functions**

$$\varphi_i(\omega_j) = \delta_{ij},$$

on specifically chosen sets of nodes  $\{\omega_j\}_j$ . The **values in the remaining nodes** are then obtained by **extending the values into the adjacent subdomains**. Examples:

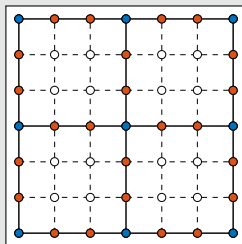
## Subdomain-based



- The  $\omega_j$  are based on nonoverl. subdomains  $\Omega_j$
- **No extensions** needed

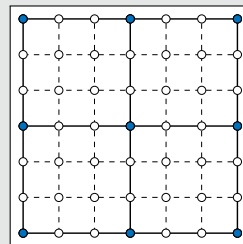
Cf. **Nicolaidis (1987)**.

## GDSW



- The  $\omega_j$  are based on **partition of the interface**
- **Energy-minimizing** exts.

## Vertex-based



- **Lagrangian**: geometric ext.
- **MsFEM**: geometric and energy-minimizing exts.
- **RGDSW**: algebraic and energy-minimizing exts.

# Learning Extension Operators

Most coarse spaces for Schwarz preconditioners are constructed based on a **characteristic functions**

$$\varphi_i(\omega_j) = \delta_{ij},$$

on specifically chosen sets of nodes  $\{\omega_j\}_j$ . The **values in the remaining nodes** are then obtained by **extending the values into the adjacent subdomains**. Examples:

## Observation 1

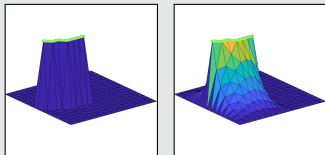
Energy-minimizing extensions

- are **algebraic**:

$$v_I = -K_{II}^{-1} K_{I\Gamma} v_\Gamma$$

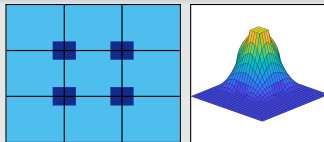
(with Dirichlet b. c.)

- can be **costly**: solving a problem in the interior



→ Improving efficiency & robustness via machine learning.

## Observation 2

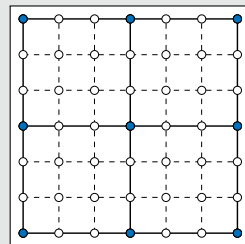


Heterogeneous:  $\alpha_{\text{light}} = 1$ ;  $\alpha_{\text{dark}} = 10^8$

The performance may **strongly** depend on extension operator:

coarse space	its.	$\kappa$
—	163	$4.06 \cdot 10^7$
Q1	138	$1.07 \cdot 10^6$
MsFEM	24	8.05

## Vertex-based



- Lagrangian**: geometric ext.
- MsFEM**: geometric and energy-minimizing exts.
- RGDSW**: algebraic and energy-minimizing exts.

This overview is **not exhaustive**:

## Coarse spaces for domain decomposition methods

- Prediction of the geometric location of adaptive constraints (adaptive BDDC & FETI-DP as well as AGDSW): [Heinlein, Klawonn, Lanser, Weber \(2019, 2020, 2021, 2021, 2021, 2022\)](#)
- Prediction of coarse basis functions: [Chung, Kim, Lam, Zhao \(2021\)](#); [Klawonn, Lanser, Weber \(2024, 2024\)](#); [Kopaničáková, Karniadakis \(2025\)](#)
- Learning interface conditions and coarse interpolation operators: [Taghibakhshi et al. \(2022, 2023\)](#)

## Algebraic multigrid (AMG)

- Prediction of coarse grid operators: [Luz et al. \(2020\)](#); [Tomasi, Krause \(2023\)](#); [Zhang et al. \(2024\)](#)
- Coarsening: [Taghibakhshi, MacLachlan, Olson, West \(2021\)](#); [Antonietti, Caldana, Dede \(2023\)](#)

An overviews of the **state-of-the-art on domain decomposition and machine learning** in early 2021 and 2023:



A. Heinlein, A. Klawonn, M. Lanser, J. Weber

**Combining machine learning and domain decomposition methods for the solution of partial differential equations — A review**  
GAMM-Mitteilungen. 2021.



A. Klawonn, M. Lanser, J. Weber

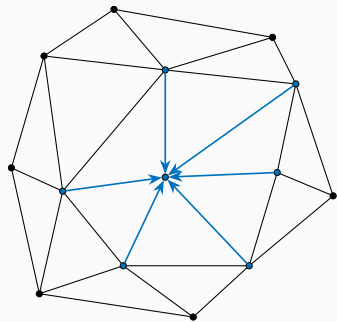
**Machine learning and domain decomposition methods – a survey**  
Computational Science and Engineering. 2024

# Prediction via Graph Convolutional Networks

**Graph neural networks (GNNs)** Gori, Monfardini, and Scarselli (2005) are a natural choice for learning on data defined over simulation meshes:

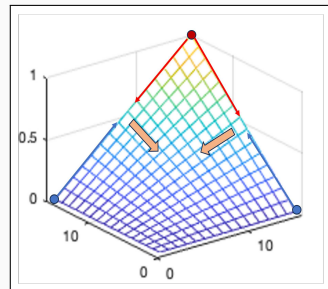
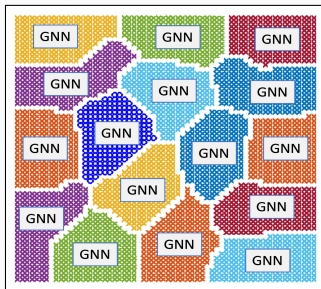
- Generalize **CNNs** LeCun (1998) to irregular, **graph-structured data**.
- Learn via **iterative aggregation** from **neighboring nodes**.
- Naturally **permutation invariant** and **geometrically robust**.

Further references: Scarselli et al. (2005), Bruna et al. (2014), Henaff et al. (2015), Defferrard et al. (2016), Kipf, Welling (2017), ...



## Local approach

- **Input:** subdomain matrix  $K_i$
- **Output:** basis functions  $\{\varphi_j^{\Omega_i}\}_j$  on the same subdomain
- Training on **subdomains with varying geometry**
- Inference on **unseen subdomains**



# Theory-Inspired Design of the GNN-Based Coarse Space

## Null space property

Any extension-based coarse space built from a partition of unity on the domain decomposition interface satisfies the **null space property necessary for numerical scalability**:

$$\sum_{\text{edges } \subset \partial\Omega_i} \text{[3D plot of a peak on an edge]} + \sum_{\text{vertices } \subset \partial\Omega_i} \text{[3D plot of a peak at a vertex]} = \text{[3D plot of a combined peak structure]}$$

## Explicit partition of unity

To **explicitly enforce** that the basis functions  $(\varphi_j)_j$  form a **partition of unity**

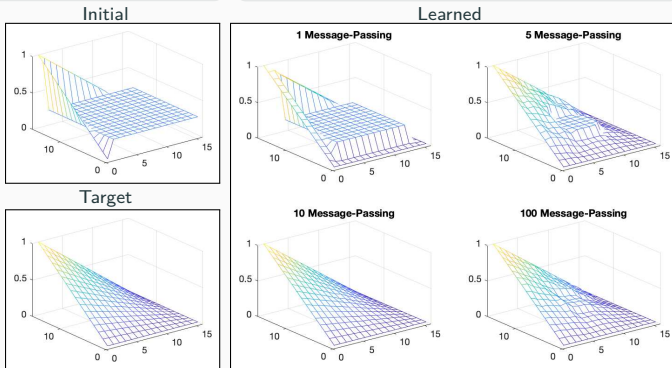
$$\varphi_j = \frac{\hat{\varphi}_j}{\sum_k \hat{\varphi}_k},$$

where the  $\hat{\varphi}_k$  are the outputs of the GNN.

## Initial and target

- **Initial function:** partition of unity that is constant in the interior
- **Target function:**
  - linear on the edges
  - energy-minimizing in the interior

→ **Information transport via message passing**

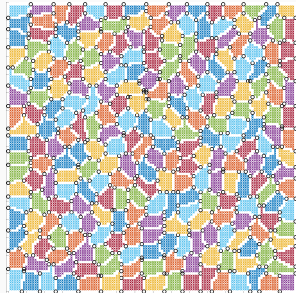


# Numerical Results for Homogeneous Laplacian – Weak Scaling Study

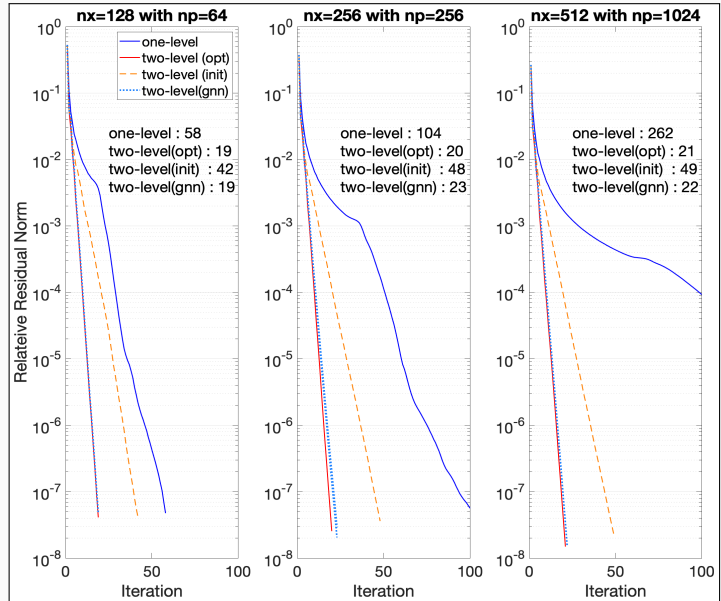
**Model problem:** 2D Laplacian model problem discretized using finite differences on a structured grid

$$\begin{aligned} -\Delta u &= 1 && \text{in } \Omega, \\ u &= 0 && \text{on } \partial\Omega, \end{aligned}$$

decomposed using **METIS**:



- The GNN has been **trained on 64 subdomains**.

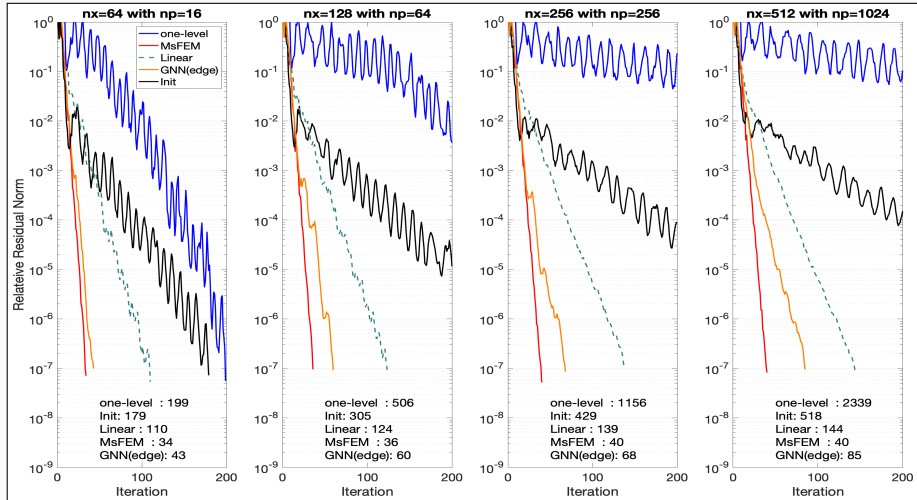


Yamazaki, Heinlein, Rajamanickam (subm. 2024)

# Numerical Results for Heterogeneous Laplacian – Weak Scaling Study

Heterogeneous Laplacian with  $\alpha_{\max}/\alpha_{\min} = 10^3$ :

$$-\nabla \cdot (\alpha(x)\nabla u(x)) = f \text{ in } \Omega = [0, 1]^2, \quad u = 0 \text{ on } \partial\Omega.$$



Yamazaki, Heinlein, Rajamanickam (subm. 2024)

# Scientific Machine Learning in Academia and Beyond:

## From Theory to Real-World Impact (in Industry)

- **Dates:** June 17, 2025, 12.30–17.30
- **Location:** Crowne Plaza Hotel, Utrecht
- **Lunch & networking:** 12.30–13.30; closing discussion & drinks to follow.
- An afternoon with **talks, case studies, and lively discussions** on advancing scientific machine learning from theory to real-world deployment — tackling core challenges like *uncertainty quantification, data assimilation, graph-based modelling, and operator learning*.
- **Confirmed plenary speakers:**
  - [Max Welling](#) (UvA, CUSP AI)
  - [Stefan Kurz](#) (ETH Zürich & Bosch)
  - [Koen Strien](#) (Ignition Computing)
  - [Maxim Pisarenco](#) (ASML)
  - [Jan Willem van de Meent](#) (UvA)



**Computational  
Science NL**

# CWI Research Semester Programme:

## Bridging Numerical Analysis and Scientific Machine Learning: Advances and Applications

**Co-organizers:** Victorita Dolean (TU/e), Alexander Heinlein (TU Delft), Benjamin Sanderse (CWI), Jemima Tabbart (TU/e), Tristan van Leeuwen (CWI)

- **Autumn School** (October 27–31, 2025):
  - [Chris Budd](#) (University of Bath)
  - [Ben Moseley](#) (Imperial College London)
  - [Gabriele Steidl](#) (Technische Universität Berlin)
  - [Andrew Stuart](#) (California Institute of Technology)
  - [Andrea Walther](#) (Humboldt-Universität zu Berlin)
  - [Ricardo Baptista](#) (University of Toronto)
- **Workshop** (December 1–3, 2025):
  - 3 days with plenary talks (academia & industry) and an industry panel
  - Confirmed plenary speakers:
    - [Marta d'Elia](#) (Atomic Machines)
    - [Benjamin Peherstorfer](#) (New York University)
    - [Andreas Roskopf](#) (Fraunhofer Institute)



Centrum Wiskunde & Informatica



**Join us for inspiring talks, hands-on sessions, and industry collaboration!**

## FROSch (Fast and Robust Overlapping Schwarz)

- FROSch is based on the **Schwarz framework** and **energy-minimizing coarse spaces**, which provide **numerical scalability** using **only algebraic information** for a **variety of applications**
- FROSch is well-integrated into the TRILINOS software framework, enabling
  - **large-scale distributed memory parallelization** and
  - **node-level performance on CPU and/or GPU architectures**

## Learning extension operators

- **Extensions** are a major component in the **construction of coarse spaces** for domain decomposition methods.
- Using **GNNs** and **known properties from the theory**, we can **learn extension operators** that lead to a **scalable coarse spaces**.

Thank you for your attention!



Topical Activity  
Group  
Scientific Machine  
Learning

